

Ergodic properties of a generic non-integrable quantum many-body system in thermodynamic limit

Tomaž Prosen

Physics Department, Faculty of Mathematics and Physics, University of Ljubljana, Jadranska 19, 1111 Ljubljana, Slovenia
(February 5, 2020)

We study a generic but simple non-integrable quantum *many-body* system of *locally* interacting particles, namely a kicked $t - V$ model of spinless fermions on 1-dim lattice (equivalent to a kicked Heisenberg XX-Z chain of 1/2 spins). Statistical properties of dynamics (quantum ergodicity and quantum mixing) and the nature of quantum transport in *thermodynamic limit* are considered as the kick parameters (which control the degree of non-integrability) are varied. We find and demonstrate *ballistic* transport and non-ergodic, non-mixing dynamics (implying infinite conductivity at all temperatures) in the *integrable* regime of zero or very small kick parameters, and more generally and important, also in *non-integrable* regime of *intermediate* values of kicked parameters, whereas only for sufficiently large kick parameters we recover quantum ergodicity and mixing implying normal (diffusive) transport. We propose an order parameter (charge stiffness D) which controls the phase transition from non-mixing/non-ergodic dynamics (ordered phase, $D > 0$) to mixing/ergodic dynamics (disordered phase, $D = 0$) in the thermodynamic limit. Furthermore, we find *exponential decay of time-correlation function* in the regime of mixing dynamics.

The results are obtained consistently within three different numerical and analytical approaches: (i) time evolution of a finite system and direct computation of time correlation functions, (ii) full diagonalization of finite systems and statistical analysis of stationary data, and (iii) algebraic construction of quantum invariants of motion, in particular the time averaged observables.

PACS numbers: 05.45.+b, 05.30.Fk, 72.10.Bg

I. INTRODUCTION

It has been a common belief for a long time, that a large system of sufficiently many interacting particles should fill uniformly the entire available phase space. This is known as *ergodic hypothesis*, one of the cornerstones of the statistical mechanics, and is a necessary assumption to justify the use of canonical ensembles and derivation of fundamental laws of statistical physics, such as transport laws (e.g. Ohm's law or Fourier's law).

However, the proof together with the precise conditions for the validity of ergodic hypothesis is still one of the most fundamental unsolved problems of theoretical physics. Even in the context of purely classical dynamics, the ergodic theory [1,2], though it is an involved and beautiful mathematical discipline, can make strong statements only for a very limited class of systems, while generic dynamical systems, especially those consisting of many particles, are far from being understood [3,4]. Even less is known about ergodic properties of generic quantum many body systems, which is precisely the objective of this paper. A closed (finite) and bounded quantum system of size L and with a finite number N of particles has a discrete spectrum, hence its time evolution is quasi-periodic, and accordingly it is non-ergodic and non-mixing, as we shall define below. However, in the thermodynamic limit (TL), of diverging size $L \rightarrow \infty$ and density of particles $\rho = N/L$ fixed, the spectrum of the quantum propagator may become continuous, and one may expect the properties of quantum ergodicity and quan-

tum mixing to set in provided the strength of non-linear interaction is sufficiently strong. In this paper we deal with general non-autonomous many-body systems with Hamiltonians $H(\tau)$ which explicitly depend on time τ . Therefore the entire Hilbert space of many-body quantum configurations (Fock space) is dynamically accessible and the micro-canonical average of an *intensive* observable represented by an operator A , reads

$$\langle A \rangle = \lim_{L \rightarrow \infty} \frac{\text{tr } A}{\text{tr } 1}. \quad (1)$$

If the system possesses a group of exact geometric or dynamical symmetries, the trace in eq. (1) may be considered only over a specific symmetry class of the Fock space w.r.t. symmetry group. For example, if the system is autonomous, energy is conserved, and eq. (1) should be replaced by the average over a specific "energy shell", or, as often, if the number N of particles (or particle density $\rho = N/L$) is preserved, then the micro-canonical average should be performed over the Fock subspace of N -particle configurations

$$\langle A \rangle_\rho = \lim_{L \rightarrow \infty} \frac{\text{tr } (A \delta_{[\rho L], N})}{\text{tr } \delta_{[\rho L], N}} \quad (2)$$

where $[x]$ is an integer part of x and $\delta_{m,n}$ is a Kronecker symbol. When we will like to keep the size L in the average (2) fixed and finite we would write $\langle A \rangle_\rho^L$. Although in this abstract discussion we would like to avoid the notion of temperature [5], one may think of (1) or (2) as canonical averages at infinite temperature $\beta = 0$.

The system is *quantum ergodic* if the time average of an arbitrary observable in Heisenberg picture $A(\tau)$ equals to the micro-canonical average $\langle A \rangle$ times a unit operator (over the corresponding desymmetrized Fock subspace)

$$\bar{A} := \lim_{T \rightarrow \infty} \frac{1}{T} \int_0^T d\tau A(\tau) = \langle A \rangle 1. \quad (3)$$

In case where one has a constant of motion, e.g. density ρ (or energy $E = H$, etc.) one should define the ergodicity through the spectral resolution of the relevant invariant operator, $\rho = \int \rho' dE_{\rho'}$, namely

$$\bar{A} = \int \langle A \rangle_{\rho'} dE_{\rho'}. \quad (4)$$

When the micro-canonical average does not depend on the eigenvalues of the symmetry operations, e.g. $\langle A \rangle_{\rho} = \langle A \rangle$, definition (4) is equivalent to a simple one (3).

Even stronger ergodic property is quantum mixing, which is defined very generally [6] as follows: The infinite ($L = \infty$) quantum many-body system is called quantum mixing if time-correlations for an arbitrary pair of quantum observables in Heisenberg representation, $A(\tau)$ and $B(\tau)$, decay to zero

$$\begin{aligned} C_{AB}(\tau) &:= \langle A(\tau)B(0) \rangle - \langle A \rangle \langle B \rangle, \\ \lim_{\tau \rightarrow \infty} C_{AB}(\tau) &= 0. \end{aligned} \quad (5)$$

Note that formula (5) implies that TL should be considered prior to the time limit, $\tau \rightarrow \infty$, since these two limits do not generally commute [6]. Again, in case of additional symmetry, mixing over separate symmetry classes can be studied; as well as *uniform mixing* over entire Fock space (which makes sense when canonical averages of A and B do not depend on eigenvalues of symmetry operations like ρ).

In Ref. [6] quantum mixing of a system of interacting bosons has been related to a hard chaos of the corresponding classical (mean field) model. However, general quantum systems need not possess the classical limit; when they do, the general definitions (3-5) go over to the correct definitions of classical ergodicity and mixing of the corresponding classical counterparts.

It is easy to see that the same implication holds as in classical mechanics [2]: Quantum mixing (5) implies quantum ergodicity (3). To see this, observe that as a simple consequence of (5), time averaged correlation function should vanish,

$$\bar{C}_{AB} := \lim_{T \rightarrow \infty} \frac{1}{T} \int_0^T d\tau C_{AB}(\tau) = 0.$$

This fact is equivalent to

$$\langle \bar{A}B \rangle - \langle A \rangle \langle B \rangle = \langle (\bar{A} - \langle A \rangle 1)B \rangle = 0.$$

Then we immediately see that observable in brackets should vanish $\bar{A} - \langle A \rangle 1 = 0$, since observable B is arbitrary. q.e.d. The last argument can be reversed, so we

see that quantum ergodicity (3) is equivalent to $\bar{C}_{AB} = 0$ for arbitrary pair A, B .

We expect that quantum mixing implies universal statistical properties of energy spectra (and also universal statistics of occupation numbers [7], matrix elements, etc). Random matrix spectral statistics have indeed been demonstrated numerically for few strongly non-integrable many-body systems [8]. On the other hand, completely integrable quantum many-body systems (having an infinite set of independent conservation laws $Q_n, n = 1, 2, 3, \dots$) are obviously non-ergodic ($\bar{Q}_n = Q_n \neq \langle Q \rangle_n 1$), and therefore non-mixing, and characterized by the universal Poissonian spectral statistics [8].

It has been pointed out recently [9,13] that integrability typically implies non-vanishing stiffness, i.e. ideal conductance with infinite transport coefficients (or ideal insulating state). Indeed, there is a direct implication of quantum mixing and quantum ergodicity on quantum transport. One should simply inspect a Kubo formula [10], which relates the real part of the transport coefficient, e.g. electric conductivity $\sigma'(\omega)$, to the cosine transform of the autocorrelation function of the electric current observable J , written for high temperatures (small β) as

$$\sigma'(\omega) = \frac{1}{2} \beta \int_{-\infty}^{\infty} \cos(\omega\tau) \langle \frac{1}{L} J(0) J(\tau) \rangle d\tau. \quad (6)$$

The transport is diffusive and the system behaves as a *normal conductor* if zero-frequency (d.c.) conductivity is finite, $\sigma'(0) < \infty$, which means that the time integral of the current-current correlation function should be finite; this is true if the system is mixing and if time correlations decay sufficiently fast, e.g. it is sufficient that $|\langle \frac{1}{L} J(0) J(\tau) \rangle| < C|\tau|^{-\alpha}$ for some $C > 0$ and $\alpha > 1$.

On the other hand, if the transport is ballistic, d.c. conductivity diverges $\sigma'(0) = \infty$ and frequency dependent conductivity can be written as a sum of delta-spike and a regularized conductivity

$$\sigma'(\omega) = D\delta(\omega) + \sigma_{\text{reg}}(\omega), \quad D = \lim_{\epsilon \rightarrow 0} \int_{-\epsilon}^{\epsilon} \sigma'(\omega) d\omega \quad (7)$$

The weight D is known as a *charge stiffness* (or Drude weight) and is proportional to the averaged current-current time correlator

$$D = \beta D_J, \quad D_A = \lim_{T \rightarrow \infty} \lim_{L \rightarrow \infty} \frac{1}{2TL} \int_{-T}^T C_{AA}^L(\tau) d\tau \quad (8)$$

Therefore, non-vanishing charge stiffness $D_J \neq 0$, meaning a ballistic electric transport, is a sufficient condition for deviation from quantum ergodicity, so D_J will be extensively used as a quantitative indicator of quantum (non)ergodicity throughout the rest of this paper.

In a generic integrable system one can find an (infinite) set of invariant *extensive* observables, the so-called conserved charges Q_n . Mazur [11] and Suzuki [12] have

proposed a ‘Parseval-like’ inequality for the time averaged autocorrelator of any extensive observable A

$$D_A \geq \sum_n \frac{|\langle \frac{1}{L}AQ_n \rangle|^2}{\langle \frac{1}{L}Q_n^2 \rangle}, \quad (9)$$

using any suitable (sub)set of conserved charges $\{Q_m\}$, such that $\langle \frac{1}{L}Q_nQ_m \rangle = 0$ if $n \neq m$. For an integrable system one therefore proves ideal (ballistic) transport ($D_J > 0$) if at least one term in an infinite sum on RHS of eq. (9) applied to the current observable $A = J$ is non-vanishing (what is typically the case) [13]. It is convenient to say that $\{Q_n\}$ is a *complete* set of conserved charges when (9) is an exact *equality* for any observable A (which is ‘square-summable’, $\langle \frac{1}{L}A^2 \rangle < \infty$).

The important and delicate question is whether non-ergodicity of an integrable system in TL can be structurally stable against generic and finite non-integrable perturbation. In this paper we will present clear numerical evidences based on various different and independent numerical methods in support of a conjecture claiming an affirmative answer to the above question.

Conjecture: Let H_λ be a continuous family of *generic infinite* quantum-many body systems with *local* interaction [14], such that H_0 is completely-integrable while H_λ are non-integrable for almost any $\lambda \neq 0$. Then, $\exists \lambda_c$, such that H_λ are *non-ergodic* and *non-mixing* for $|\lambda| < \lambda_c$.

One important consequence of the above Conjecture would be a large class of not only integrable but also nearly-integrable many-body systems for which ideal transport and infinite conductance would be expected.

In Sec. II we define a two parametric family of generic non-integrable many-body systems [15], namely a kicked t-V model of interacting spinless fermions, or equivalently, a kicked Heisenberg XX-Z spin- $\frac{1}{2}$ chain, and describe the basic properties of the model. In Sec. III we show how efficient explicit time evolution of the above model of finite but quite large size L can be computed, and present results on extensive numerical computation of time correlation functions. By letting the size L to increase and inspecting TL, we clearly identify two regimes of quantum motion: *non-mixing* regime for small and intermediate values of kick parameters where time-correlation functions typically saturate to constant non-vanishing values, and *exponentially mixing* regime for sufficiently large values of kick parameters where time correlation functions decay *exponentially*. As a complementary approach to direct time evolution (time domain) we perform, in Sec. IV, complete diagonalization of stationary problem (frequency domain) for finite sizes L . Using stationary data we have computed and analyzed short-range and long-range quasi-energy level statistics. By means of matrix elements of the current observable J we have also directly computed the conductance and the charge stiffness D_J . The obtained results are in quantitative agreement with a direct time evolution (Sec. III).

In Sec. V we outline completely different and independent method of computing time-averaged observables, and quantitative indicators of quantum ergodicity such as the charge stiffness D_J , by making use of extensive computerized Lie algebra. This third method, in contrast to other two, refers directly to infinite systems (infinite lattices $L = \infty$) and, again, gives compatible results. In Sec. VI we give more arguments in support of our Conjecture by discussing relevant published and unpublished results and conclude.

II. THE MODEL

No general analytical methods exist to deal with dynamics of non-integrable quantum many-body systems. A beautiful solution theory based on inverse scattering and algebraic Bethe ansatz [16] is unfortunately applicable only to a limited class of very special, namely completely integrable many-body systems. Therefore one is left to numerical experiment to learn about dynamics of generic quantum systems, encouraged with the fact that numerical and experimental investigations of dynamical systems of one or few particles has been a very fruitful area of research (known as Quantum Chaos) over the past twenty years [17]. However, one should be very careful in picking out the toy model, since the fact, that the dimensionality of the Hilbert space (Fock space of quantum many-body states) grows exponentially with increasing system size L , makes a serious quantitative study of TL almost prohibitive. Here we propose the simplest many-body system that we can think of: one dimensional lattice of spinless fermions of size L , and for the reasons which will become clear in the next section, we decide to break integrability by taking time-dependent interaction which is switched on periodically by means of δ -kicks. Therefore, the time-dependent Hamiltonian of our “kicked t-V model” (KtV) [15] reads

$$H(\tau) = \sum_{j=0}^{L-1} \left[-\frac{1}{2}t(c_j^\dagger c_{j+1} + h.c.) + \delta_p(\tau) V n_j n_{j+1} \right]. \quad (10)$$

c_j^\dagger, c_j are fermionic creation and annihilation operators satisfying canonical anticommutation relations $[c_j, c_k]_+ := c_j c_k + c_k c_j = 0, [c_j^\dagger, c_k]_+ = \delta_{jk}, n_j = c_j^\dagger c_j$ are number operators, and periodic boundary conditions are imposed $c_L \equiv c_0$. $\delta_p(\tau) = \sum_{m=-\infty}^{\infty} \delta(\tau - m)$ is a periodic δ -function. We use units in which \hbar = (time between collisions) = (lattice spacing) = 1. The hopping amplitude t and interaction strength V are independent (kick) parameters. An important and useful property of kicked systems like (10) is the fact that the evolution propagator over one period (Floquet operator) factorizes into the product of kinetic and potential part

$$U = \hat{\mathcal{T}} \exp \left(-i \int_{0^+}^{1^+} d\tau H(\tau) \right)$$

$$= \exp(-iW) \exp(-iT), \quad (11)$$

$$T = -\frac{1}{2}t \sum_{j=0}^{L-1} \left(e^{i\phi} c_{j+1}^\dagger c_j + e^{-i\phi} c_j^\dagger c_{j+1} \right), \quad (12)$$

$$W = V \sum_{j=0}^{L-1} n_j n_{j+1}. \quad (13)$$

We have used a Pierels phase ϕ in order to introduce a particle current

$$J = (i/t)U^\dagger(\partial/\partial\phi)U|_{\phi=0} = \frac{1}{2}i \sum_{k=0}^{L-1} \left(c_j^\dagger c_{j+1} - c_{j+1}^\dagger c_j \right) \quad (14)$$

(which is divided by t for convenience); elsewhere we put $\phi := 0$. Note that the kinetic energy T as well as the current J are *diagonal* in momentum representation

$$T = t \sum_{k=0}^{L-1} (1 - \cos(sk)) \tilde{n}_k, \quad (15)$$

$$J = \sum_{k=0}^{L-1} \sin(sk) \tilde{n}_k, \quad (16)$$

where $s = 2\pi/L$, while tilde refers to momentum representation of field operators

$$\tilde{c}_k = L^{-1/2} \sum_{j=0}^{L-1} \exp(isjk) c_j, \quad \tilde{n}_k = \tilde{c}_k^\dagger \tilde{c}_k. \quad (17)$$

Using a well known Jordan-Wigner transformation [18] one can map 1-dim lattice of spinless fermions to a spin- $-\frac{1}{2}$ chain described by Pauli operators $\sigma_j^\pm = (\sigma_j^x \pm i\sigma_j^y)/\sqrt{2}, \sigma_j^z$, namely

$$\begin{aligned} \sigma_j^\pm &= \sqrt{2} c_j^\dagger \exp\left(i\pi \sum_{j'=0}^{j-1} n_{j'}\right) \\ \sigma_j^z &= 2n_j - 1, \end{aligned} \quad (18)$$

which satisfy canonical commutation relations

$$[\sigma_j^\mu, \sigma_k^\nu] = i \sum_\eta \epsilon_{\mu\nu\eta} \sigma_j^\eta \delta_{jk}, \quad \mu, \nu, \eta \in \{x, y, z\}.$$

In fact, Jordan-Wigner transformation (18) maps KtV model on a kicked Heisenberg XX-Z chain

$$H(\tau) = T + \delta_p(\tau)W, \quad (19)$$

$$T = \frac{1}{4}t \sum_{j=0}^{L-1} (\sigma_j^x \sigma_{j+1}^x + \sigma_j^y \sigma_{j+1}^y), \quad (20)$$

$$W = \frac{1}{4}V \sum_{j=0}^{L-1} (\sigma_j^z \sigma_{j+1}^z + 2\sigma_j^z). \quad (21)$$

The last term of potential (21) is irrelevant since the total z -spin $S_z = \sum_{j=0}^{L-1} \sigma_j^z = N - \frac{1}{2}L$ is a constant of motion, $[U, S_z] = 0$.

Interaction strength V is *cyclic parameter* $V \equiv V \pmod{2\pi}$, since the spectrum of W/V is a set of integers (see 13). KtV model is integrable/solvable in three special (limiting) cases:

1. $t = 0$, 1-dim Ising model,
2. $V = 0 \pmod{2\pi}$, 1-dim free fermions, or equivalently, 1-dim Heisenberg XX $\frac{1}{2}$ -spin chain,
3. $tV \rightarrow 0$ and $\Delta = t/V$ finite, (continuous-time) 1-dim Heisenberg XXZ $\frac{1}{2}$ -spin chain.

For $t \neq 0, V \neq 0 \pmod{2\pi}$, KtV is expected to be non-integrable, possibly quantum ergodic and mixing.

To conclude this section, let us list the symmetries of a general KtV model (for arbitrary t and V): In addition to the trivial conservation law, namely the number or density of particles

$$N = \sum_{j=0}^{L-1} n_j, \quad \rho = \frac{N}{L}, \quad [U, N] = 0, \quad (22)$$

and the total quasi-momentum $K \in \{0, 1, \dots, L-1\}$ which is defined as an eigenvalue of a unitary translational symmetry operation S

$$S = \exp(isK) = \exp\left(is \sum_{k=0}^{L-1} k \tilde{n}_k\right), \quad [U, S] = 0, \quad (23)$$

the KtV model has two (geometric) ‘reflection’ symmetries, namely the *parity*

$$\hat{P} : c_j \rightarrow c_{L-j}, \quad \hat{P}U = U\hat{P}, \quad \hat{P}^2 = \hat{1}, \quad (24)$$

and, for even size L , the particle-hole transformation

$$\hat{R} : c_j \rightarrow (-1)^j c_j^\dagger, \quad \hat{R}U = U\hat{R}, \quad \hat{R}^2 = \hat{1}. \quad (25)$$

Note on notation: Symbols wearing a *hat* $\hat{\cdot}$ denote linear transformations over the operator space of quantum observables.

III. FIRST METHOD: DIRECT TIME EVOLUTION AND CORRELATION FUNCTIONS

For a fixed size L and fixed number of fermions N , a unitary quantum many-body map U (11) acts over a Fock space of dimension

$$\mathcal{N} = \binom{L}{N} = \frac{L!}{N!(L-N)!}. \quad (26)$$

Dynamics of a given initial many-body state $|\psi(0)\rangle$ is given by a simple iteration of the Floquet map

$$|\psi(m)\rangle = U|\psi(m-1)\rangle = U^m|\psi(0)\rangle. \quad (27)$$

Many body states $|\psi\rangle$ can be expanded in a complete basis of the Fock space (of Slater determinants), for which we may choose either the *position states*, labelled by sets of N ordered integers $\vec{j} = (j_1, \dots, j_N)$

$$|\vec{j}\rangle = c_{j_1} \cdots c_{j_N} |0\rangle, \quad 0 \leq j_1 \leq \dots \leq j_N < L, \quad (28)$$

or the *momentum states*, labeled by sets of N ordered integers \vec{k}

$$|\vec{k}\rangle = \tilde{c}_{k_1} \cdots \tilde{c}_{k_N} |0\rangle, \quad 0 \leq k_1 \leq \dots \leq k_N < L. \quad (29)$$

An important observation, implicitly made already in previous section (11,13,15), is that kinetic propagator $\exp(-iT)$ is *diagonal* in momentum representation while potential propagator $\exp(-iW)$ is *diagonal* in position representation

$$\begin{aligned} U_{\vec{k}, \vec{k}'}^T &:= \langle \vec{k} | \exp(-iT) | \vec{k}' \rangle \\ &= \delta_{\vec{k}, \vec{k}'} \exp \left(it \sum_{n=1}^N (\cos(sk_n) - 1) \right), \end{aligned} \quad (30)$$

$$\begin{aligned} U_{\vec{j}, \vec{j}'}^W &:= \langle \vec{j} | \exp(-iW) | \vec{j}' \rangle \\ &= \delta_{\vec{j}, \vec{j}'} \exp \left(-iV \sum_{n, n'=1}^N \delta_{j_n, j_{n'}+1} \right). \end{aligned} \quad (31)$$

Therefore, one may formulate a very efficient algorithm to perform explicit time evolution of many-body states, provided that it is possible to switch between the two representations (28) and (29) as efficiently as in the problem of one kicked quantum particle $N = 1$, e.g. kicked rotor [19] or kicked Harper model [20], namely by means of Fast Fourier Transformation (FFT) algorithm. Indeed, we succeeded to develop a fast algorithm which performs such anti-symmetrized multi-dimensional discrete Fourier transformation

$$F_{\vec{j}, \vec{k}} = \langle \vec{j} | \vec{k} \rangle \quad (32)$$

in roughly $\mathcal{N} \log_2 \mathcal{N}$ Floating Point Operations (FPO). It is based on a factorization of L -site discrete Fourier transformation into the product of $\sim L \log_2 L$ 2-site transformations parametrized with 2×2 sub-matrices $(\alpha, \beta; \gamma, \delta)_{jj'}$, which are successively applied to creation operators, $(c_j^\dagger, c_{j'}^\dagger) \leftarrow (\alpha c_j^\dagger + \beta c_{j'}^\dagger, \gamma c_j^\dagger + \delta c_{j'}^\dagger)$, in all slater determinants $\Pi_n c_{j_n}^\dagger |0\rangle$ which contain a particle at sites j or j' . (One should be careful in dealing with fermionic signs of Slater determinants when sorting the factors in the product $\Pi_n c_{j_n}^\dagger |0\rangle$). In case when $L = 2^p$, factorization of FFT to a chain of 2-site (in such case unitary) transformations is easily deduced by inspecting a conventional FFT algorithm (such as the one implemented in [21]), while for more general lattice sizes (we have so far implemented our Fermionic FFT - FFFT algorithm

also for $L = 10, 12, 15, 20, 24, 30, 40$) we factorized the optimal schemes developed by Winograd [22]. Our FFFT algorithm requires almost no extra storage apart from a vector of \mathcal{N} c-numbers where quantum many-body state is stored. Therefore, the map (11) is iterated on a vector $\psi_{\vec{k}}(m) = \langle \vec{k} | \psi(m) \rangle$, using the matrix composition

$$U = F^* U^W F U^T \quad (33)$$

in roughly $2\mathcal{N} \log_2 \mathcal{N}$ FPO per time step which is by far superior to ‘brute-force’ methods based on complete diagonalization of U and expansion of time-evolving state $|\psi(m)\rangle$ in terms of eigenstates of U .

Let us now consider time autocorrelation functions of two ‘generic’ observables, namely current J and rescaled traceless kinetic energy T'

$$\begin{aligned} C_J^L(m) &:= \frac{1}{L} \langle J(0) J(m) \rangle_\rho^L \\ C_T^L(m) &:= \frac{1}{L} \langle T'(0) T'(m) \rangle_\rho^L, \quad T' = \frac{1}{t} T - N \end{aligned} \quad (34)$$

$J(m) = U^{\dagger m} J U^m$, $T'(m) = U^{\dagger m} T' U^m$. Note that $\langle J \rangle_\rho^L = \langle T' \rangle_\rho^L = 0$. These two observables belong to different symmetry classes with respect to parity operation

$$\hat{P}J = -J\hat{P}, \quad \hat{P}T' = T'\hat{P}, \quad (35)$$

so we choose both to check whether many-body dynamics depends of the symmetry class w.r.t. ‘reflection’ symmetry. Conveniently, both observables, J and T' , are diagonal in momentum representation,

$$J|\vec{k}\rangle = J_{\vec{k}}|\vec{k}\rangle, \quad J_{\vec{k}} = \sum_{n=1}^N \sin(sk_n), \quad (36)$$

$$T'|\vec{k}\rangle = T'_{\vec{k}}|\vec{k}\rangle, \quad T'_{\vec{k}} = -\sum_{n=1}^N \cos(sk_n), \quad (37)$$

so the time auto-correlation functions can be computed from time evolution of a (complete) set of \mathcal{N}' ($= \mathcal{N}$) initial momentum states \vec{k}'

$$C_A(m) = \frac{1}{L\mathcal{N}'} \sum'_{\vec{k}'} A_{\vec{k}'} \sum_{\vec{k}} A_{\vec{k}} p_{\vec{k}\vec{k}'}(m) \quad (38)$$

where A is any observable which is diagonal in momentum basis (here either J or T') and

$$p_{\vec{k}\vec{k}'}(m) = |\langle \vec{k} | \psi(m) \rangle|^2 = |\langle \vec{k} | U^m | \vec{k}' \rangle|^2. \quad (39)$$

When dimensionality \mathcal{N} becomes prohibitively large we suggest to estimate the microcanonical averages (34) by taking a smaller $1 \ll \mathcal{N}' \ll \mathcal{N}$ but uniformly random sample of \mathcal{N}' initial states $|\vec{k}'\rangle$, $\langle \cdot \rangle = \frac{1}{\mathcal{N}'} \sum'_{\vec{k}'} \langle \vec{k}' | \cdot | \vec{k}' \rangle (1 + \mathcal{O}(1/\sqrt{\mathcal{N}'}))$. Therefore, numerical computation of correlation function $C_A(m)$ for $m = 1, \dots, M$ can be performed in $\sim (2M\mathcal{N}'\mathcal{N} \log_2 \mathcal{N})/L$ FPO. Reduction for a

factor $1/L$ w.r.t. naive FPO count is due to translational symmetry (23), since one can simultaneously simulate the dynamics of L different states with different values of the conserved total momentum $K = \sum_{n=1}^N k'_n \pmod{L}$.

Let us for the time being fix the density of particles $\rho = N/L = 1/4$. We have performed extensive numerical computations of time-correlation functions (by means of explicit time evolution (38)), for sizes $L = 8, 12, 16, 20, 24, 32$ (at $L = 32$ the dimensionality of Fock subspace is $\mathcal{N} = 10518300$), and systematically scanned the parameter space (t, V) . We have clearly identified two regimes where we were able to probe the TL, i.e. where time-correlation functions turned out to be stable against the variation of the system size L :

(i) Quantum ergodic and mixing regime for sufficiently large value of parameter t and for any value of parameter V (away from ‘integrable axis’ $V = 0 \pmod{2\pi}$). In this regime, time correlation functions are rapidly decreasing (Case $t = V = 4$ is shown in Fig.1). However, for a finite size L the quantum system is almost never mixing, so correlation functions saturate, on a time scale $\mu(L)$, to a small but finite value of the stiffness

$$D_A^L = \lim_{M \rightarrow \infty} \frac{1}{2M+1} \sum_{m=-M}^M C_A^L(m) \quad (40)$$

(Here $A = J$ or T' .) In order to avoid transient behavior at small times m and incorporating the time reversal symmetry, $C_A^L(m) = C_A^L(-m)$, the time averages like (40) have been numerically estimated as $D_A^L = \frac{1}{M'+1} \sum_{m=M'}^{2M'} C_A^L(m)$. The sufficiently large averaging time scale $\{M' \dots 2M'\} = \{30 \dots 60\}$ for all sizes $L \leq 32$ (and most values of parameters t, V) has been determined by direct inspection of the correlation functions (see Fig.1). In Fig.2 we plot correlation functions $C_J^L(m)$ for $t = V = 4$ in semi-log scale, and show that, as the size L is increased, the saturation (Thouless) time scale $\mu(L)$ increases, roughly as $\mu(L) \sim L$. The Thouless time $\mu(L)$ clearly diverges in TL. Furthermore, Fig.2 gives clear numerical evidence (further supported by results shown in Figs.4,5) of the *exponential* decay of time correlation functions in TL (or for times smaller than $\mu(L)$ in a system of finite size L)

$$C_A(m) \propto \exp(-\lambda_A m), \quad m \gg 1. \quad (41)$$

Henceforth, the stiffness should also vanish exponentially $D_A^L \sim \exp(-\lambda_A L)$ as one approaches TL (Such behavior has been observed also in Ref. [9] indicating an exponential mixing in the system studied there [9]). Indeed, in Fig.3 we examine $1/L$ scaling of the charge stiffness D_J^L which is (here shown for $t = V = 4$ and $t = V = 2$) a clear indication of ergodic and mixing behavior in TL, $D_J^\infty = 0$. In this regime, in TL, Kubo conductivity $\sigma'(\omega = 0) = \frac{1}{2}\beta \sum_{m=-\infty}^{\infty} C_J(m)$ is finite, $\sigma'(0) < \infty$, and the transport is dissipative. Fur-

ther, as shown in [15], time averaged current of arbitrary initial momentum state $|\vec{k}'\rangle$ averages to zero $\bar{J}_{\vec{k}'} = \lim_{M \rightarrow \infty} (1/M) \sum_{m=1}^M \langle \vec{k}' | J(m) | \vec{k}' \rangle = 0$, and arbitrary initial momentum state $|\vec{k}'\rangle$ explores entire accessible Fock space, i.e. $\langle \vec{k}' | U^m | \vec{k}' \rangle$ are uniformly Gaussian random when the discrete time m is sufficiently large, say larger than the quantum mixing time.

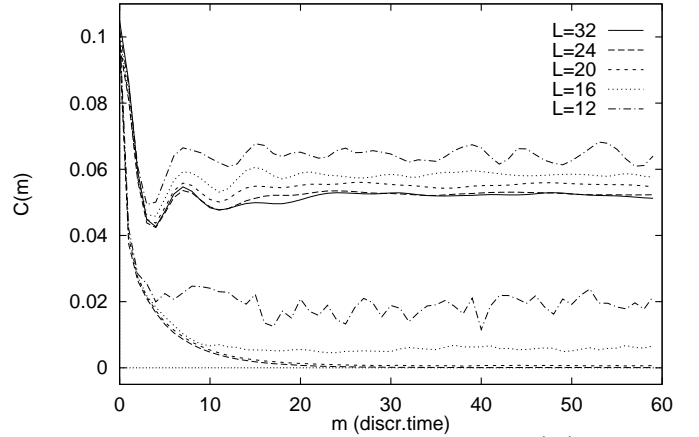


FIG. 1. Current autocorrelation function $C_J(m)$ against discrete time m for quantum ergodic ($t = V = 4$, lower set of curves for various sizes L) and intermediate regime ($t = V = 1$, upper set of curves) with density $\rho = \frac{1}{4}$. Averaging over entire Fock space is performed, $\mathcal{N}' = \mathcal{N}$, for $L \leq 20$, whereas random samples of $\mathcal{N}' = 12000$, and $\mathcal{N}' = 800$ initial states have been used for $L = 24$, and $L = 32$, respectively.

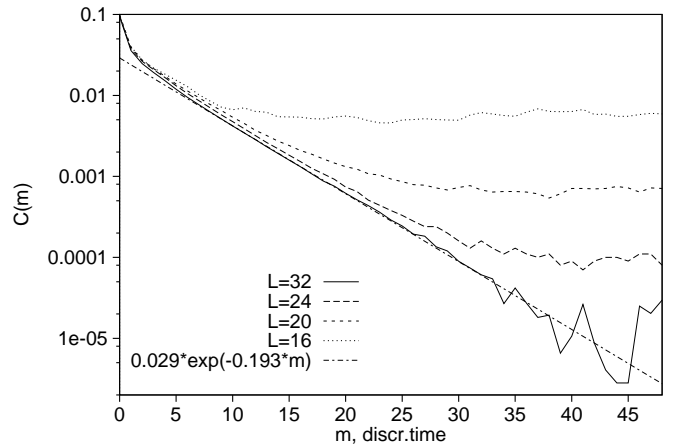


FIG. 2. The lower set of curves ($t = V = 4$) of Fig.1 in semi-log scale. To emphasize the exponential correlation decay we plot also the best exponential fit to the tail of $C_J^{L=32}(m)$ (dash-dotted line).

(ii) Non-ergodic and Non-mixing regime for parameter $t \sim 1$ (or smaller) and any value of parameter V . Here time correlation functions $C_A(m)$ do not decay to zero but saturate, around a constant typically non-vanishing and positive value of the stiffness $D_A^L > 0$ (40), on a

short time scale which *does not* depend on the size L (for sufficiently large sizes L). In Fig.1 we plot time correlation functions $C_J(m)$ for $t = V = 1$. Please observe indeed very weak dependence on the size L . In Fig.3 we also show $1/L$ scaling of charge stiffness D_J^L for the cases $t = V = 1$ and $t = 1, V = 2$ which clearly indicate a finite extrapolated (to $1/L = 0$) thermodynamic value of the stiffness. This is a clear evidence of non-mixing and non-ergodic behavior in thermodynamic limit. Since in this parameter ranges KtV model is also non-integrable, we sometimes refer to this regime as an *intermediate quantum dynamics*. This behavior corresponds to ideal, ballistic transport with infinite Kubo conductivity $\sigma = \infty$. Furthermore, in [15] it has been shown that in this intermediate regime, time averaged (persistent) current is *non-vanishing* and *proportional* to the initial current $J_{\vec{k}'}$, $\bar{J}_{\vec{k}'} = \alpha J_{\vec{k}'}$, $\alpha = 2D_J/[\rho(1 - \rho)]$ (which is the most direct probe of ideal, ballistic transport), and that an arbitrary time-evolving initial momentum state $U^m|\vec{k}'\rangle$ remain strongly localized in a non-trivial subregion of dynamically accessible Fock space.

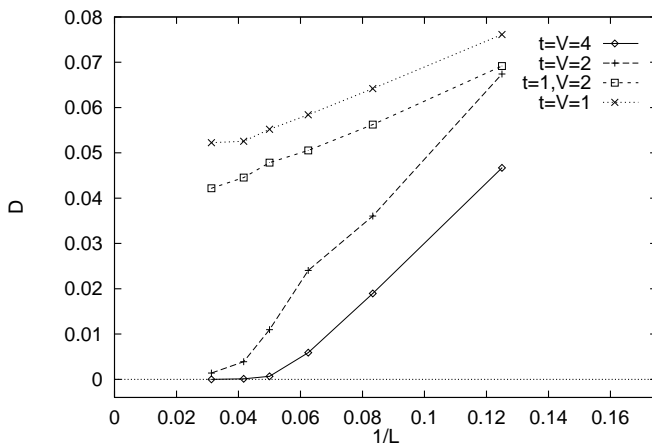


FIG. 3. Stiffness D_J vs. $1/L$ at constant density $\rho = \frac{1}{4}$ and for different values of control parameters in quantum mixing/ergodic, $t = V = 4$ and $t = V = 2$, and intermediate, $t = 1, V = 2$ and $t = V = 1$, regime. Other parameters are the same as in Fig.1

One may use a charge stiffness of an infinite system D_J^∞ as an order parameter controlling the *dynamical phase transition* from a disordered phase (quantum ergodic/mixing dynamics) characterized by $D_J^\infty = 0$ to an ordered phase (non-ergodic/non-mixing dynamics) characterized by $D_J^\infty > 0$. The transition point is characterized by diverging correlation time (or mixing time) scale, λ_J^{-1} , which diverges when one approaches the transition from above, say, with parameter t decreasing towards certain critical curve $t_c(V)$. Of course, in the ordered phase, $t < t_c(V)$, $D_J^\infty > 0$, the time-correlations have infinite range, $C_A(\infty) \neq 0$. The transition is illustrated in Figs.4,5 by plotting correlation functions

for both observables, $C_J(m)$ (Fig.4) and $C_T(m)$ (Fig.5), for different values of parameter t and fixed parameter $V = 2$. An estimate of the critical parameter here is $1.4 < t_c(V = 2) < 1.5$. Observe the exponential decay of correlations in all cases, except possibly at very small times where other, smaller time scales may become important.

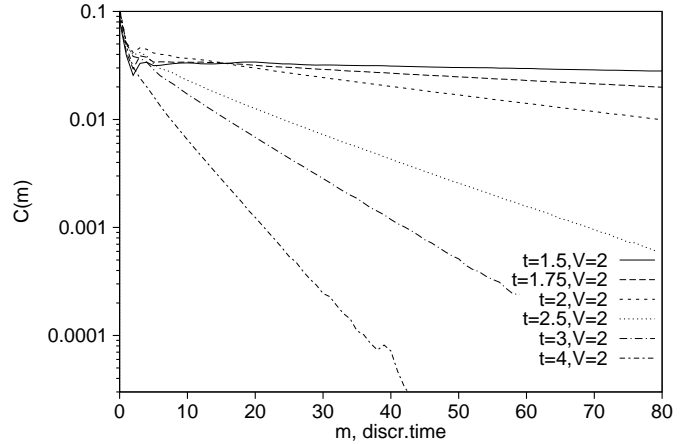


FIG. 4. Current auto-correlation functions $C_J^{L=32}(m)$ for different values of parameter t (see legend) and fixed value of parameter V . $\rho = 1/4$.

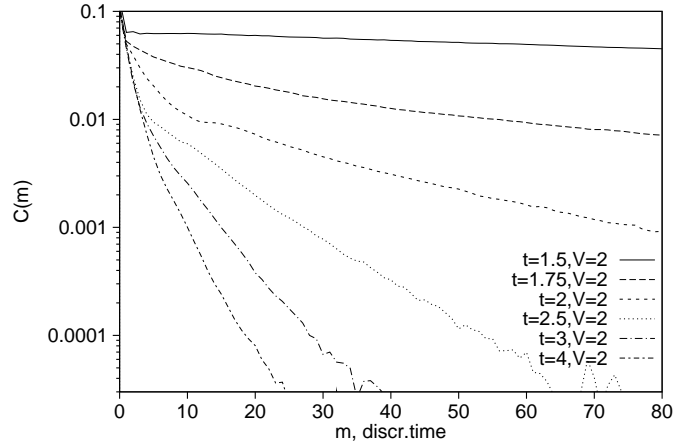


FIG. 5. Kinetic auto-correlation functions $C_T^{L=32}(m)$ for different values of parameter t (see legend) and fixed value of parameter V . $\rho = 1/4$. Note that the same scale is used than in previous Fig.4.

IV. SECOND METHOD: EXACT DIAGONALIZATION OF STATIONARY PROBLEM OF FINITE SIZE

In a more complete but brute-force approach one may try to exactly diagonalize the matrix of a one-period evolution (Floquet) propagator U for a finite size L and compute interesting dynamical quantities, such as conductivity $\sigma'(\omega)$ and stiffness D_A^L directly from the spectrum $\{\varphi_n\}$ and the set of eigenstates $\{|n\rangle\}$ of KtV map

U .

$$U|n\rangle = \exp(-i\varphi_n)|n\rangle, \quad n = 1 \dots \mathcal{N}. \quad (42)$$

Again, it is easiest to work in the momentum basis (29) and to use the translational symmetry to decompose the matrix $U_{\vec{k},\vec{k}'}$ into blocks (with fixed value of the total quasi-momentum K) of dimension $\mathcal{N}_K \approx \mathcal{N}/L$. Only for blocks with $K = 0$ and $K = L/2$ (if L is even) the parity operation $\hat{\mathcal{P}}$ (24) commutes with the translation S (23), and may be used to further reduce the dimensionality of irreducible block by factor 2. The matrix $U_{\vec{k},\vec{k}'}$ (for fixed K) has been computed, by means of a decomposition (33) and FFT algorithm, in roughly $(\mathcal{N}/L)^2 \log_2 \mathcal{N}$ FPO, and further diagonalized by means of standard routines in roughly $(\mathcal{N}/L)^3$ FPO giving a set of quasi-energies $\{\varphi_n\}$ and eigenstates $\langle \vec{k}|n\rangle$.

A. Spectral statistics

In the so called Quantum Chaology of simple (few) body non-integrable system there is a famous Conjecture of Bohigas, Giannoni and Schmit [23], supported by numerous numerical [24] and theoretical arguments [25], claiming that hard chaos (ergodicity, mixing and positive Lyapunov exponents) of a classical counterpart results in a universal statistical properties of system's (quasi)energy spectrum given by the appropriate ensemble of random matrices (Random Matrix Theory [26], RMT). On the other hand, integrable classical dynamics results in universal Poissonian statistics of (locally) uncorrelated (quasi)-energy levels [27]. Intermediate statistics, which are neither RMT nor Poissonian, are found [28,29] for systems whose classical dynamics is intermediate (mixed) with regular and chaotic motion coexisting in phase space. The connection between integrability/non-integrability and statistics has recently been investigated also in few well known examples of non-linear many-body systems (correlated fermions or interacting spin chains) which do not possess a well defined classical limit [8]. It has been shown that quantum integrability, or (strong) non-integrability, of the quantum many-body model again correspond to Poissonian, or RMT, behavior of level statistics, respectively. No attempt has been made there [8], however, to understand the intermediate situation, or the thermodynamic limit.

Inspired by Quantum Chaos we have analyzed the statistical properties of the quasi-energy spectrum $\{\varphi_n\}$ of KtV model and searched for signatures of ergodicity and mixing of the underlying quantum many-body dynamics in TL. For comparison with other results, the density will be again fixed to $\rho = 1/4$ in the numerical presentation which follows.

First, we have analyzed the common short-range statistic, namely the integrated (cumulative) nearest neighbor level spacing distribution, $W(S)$, giving the probability

that a random normalized spacing between two adjacent eigenphases $S_n = \frac{\mathcal{N}}{2\pi L}(\varphi_{n+1} - \varphi_n)$ is smaller than S

$$W(S) = \frac{1}{\mathcal{N}'} \sum_n' \theta(S - S_n). \quad (43)$$

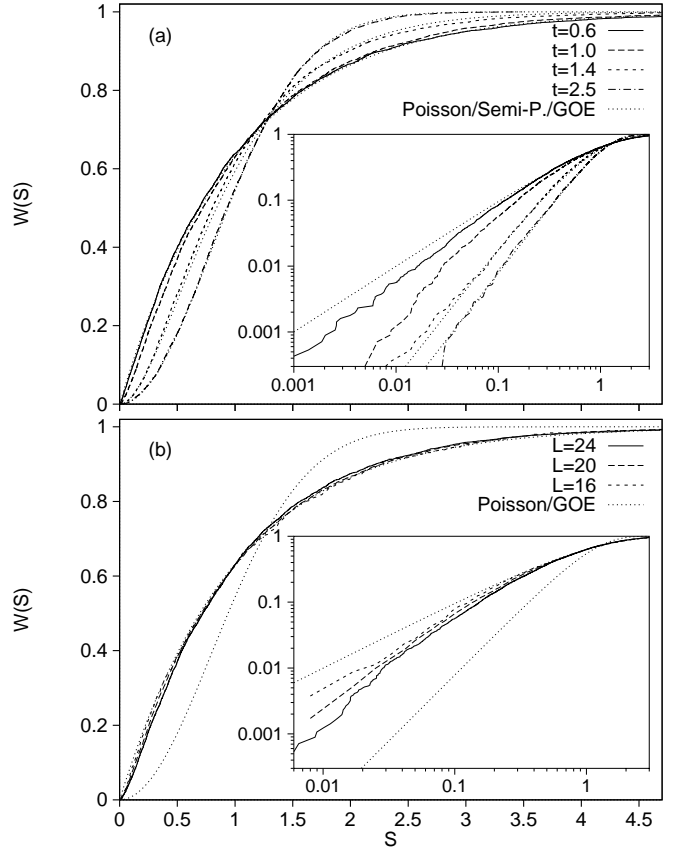


FIG. 6. Cumulative quasi-level spacing distributions $W(S)$ for quarter-filled $\rho = 1/4$ KtV model. In (a) we plot $W(S)$ for several different values of parameter t and fixed parameter V (see legend) covering the mixing/non-mixing transition, and for maximal computable size $L = 24$. With dotted curves we plot for comparison the theoretical, Poissonian, Semi-Poissonian, and Wigner (COE), distributions. In (b) we show $W(S)$ for fixed kick parameters $t = 1, V = 2$, and for different sizes $L = 16, 20, 24$. In the insets we plot the same objects in log-log scale to emphasize the small spacing behavior. Please observe the trend towards linear repulsion (quadratic for $W(S \rightarrow 0) \propto S^2$), even in intermediate regime.

For moderate values of the size $L \leq 20$, the average in (43) has been computed over all $\mathcal{N}' = \mathcal{N}$ states from all L blocks (symmetry classes) of constant quasi-momentum K . (Note that blocks for $K = K'$ and $K = L - K'$ are related by a parity transformation (24) and give identical (sub)spectra, so one has to diagonalize only $[L/2 + 1]$ different blocks of matrix $U_{\vec{k},\vec{k}'}$.) However, for larger size $L = 24$ we have already $\mathcal{N}_K \approx 5608$, so we averaged only over one class of fixed quasi-momentum, namely $K = 1$,

$\mathcal{N}' = \mathcal{N}_1 \approx \mathcal{N}/L$. (We have carefully checked that the statistical properties of partial subspectra are independent of the symmetry class labeled by quasi-momentum K .)

In Fig.6a we show $W(S)$ for size $L = 24$ and several different values of parameter t (and fixed $V = 2$) covering the transition from non-ergodic to ergodic/mixing quantum dynamics. We find almost Poissonian behavior $W_P(S) = 1 - \exp(-S)$ for small t and excellent RMT behavior $W_{\text{COE}}(S) = 1 - \exp(-\pi S^2/4)$ (Wigner surmise approximating the statistics of the infinitely-dimensional Circular Orthogonal Ensemble COE [26], due to time-reversal symmetry) for $t > t_c(V)$. In the (more interesting) region of intermediate dynamics $1 \sim t < t_c(V)$ we find intermediate statistics interpolating between Poissonian and COE (see Fig.6). Interestingly, level statistics close to the critical point (for $t = 1.4, V = 2$) seems to be well captured by the so-called Semi-Poisson model $W_{\text{SP}}(S) = 1 - (1 + 2S) \exp(-2S)$ [30] which has been recently used to model the critical level statistics of 3D Anderson model [31]. Since it is impossible to make statements about TL of level statistics, based on results for a fixed size $L = 24$, we show in Fig.6b the dependence of $W(S)$ on the size L , for fixed parameters $t = 1, V = 2$ (non-ergodic dynamics). Although the intermediate $W(S)$ statistic is closer to Poissonian than to COE, it moves towards COE as we approach TL (increase L). This fact eliminates possible fears of accidental integrability of KtV model in the claimed intermediate regime.

Second, we have analyzed the long-range spectral statistics, namely the number variance

$$\Sigma^2(S) = \langle n(S)^2 \rangle - S^2, \quad (44)$$

giving the variance of the number $n(S)$ of normalized (unfolded) levels $\frac{N}{2\pi L} \varphi_n$ in a randomly chosen interval of length S (Note that $\langle n(S) \rangle = S$.) For Poissonian and COE model we expect $\Sigma_P^2(S) = S$ and $\Sigma_{\text{COE}}^2(S) \approx (2/\pi^2) \log(2\pi S)$, respectively. Here, one should note huge degeneracies in the integrable limit $t = 0$ of Ising model (which are quite-common in integrable quantum many-body models in general). For small kick parameters t , we hence find stronger-than-Poissonian level clustering causing faster-than-linear growth of $\Sigma^2(S)$ (Fig.7a). For finite size $L = 24$, strong level clustering affects also long-range statistics in the range with mixing dynamics in TL, namely for $t = 2.5$ we find good agreement with COE statistics only for relatively small spectral ranges $S \leq S_{\text{max}} \sim 10^1$. It has been checked, however, that the agreement with COE improves, to hold on longer quasi-energy ranges (S_{max} increases), as either the kick-parameter t or the size L are increased. In the intermediate regime $1 \sim t < t_c(V)$, number variance approaches that of an uncorrelated sequence, $\Sigma^2(S) \sim S$, as we approach TL (see Fig.7b for case $t = 1, V = 2$). However, for finite L , the phenomenon of saturation sets in [32], namely when the scaled energy range $S = S^*$ is of the order of the density of states

$$S^* = 0.5\mathcal{N}/L, \quad (45)$$

i.e. when the energy range S^* becomes comparable to the length of quasi-energy spectrum. Numerical factor 0.5 in (45) is of phenomenological origin. Indeed for data of Fig.7, for $L = 12, 16, 20, 24$, the maxima of number variance lie at 9, 55, 390, 2800, whereas theoretical values of S^* (45) are 9.1, 56.9, 387.5, 2804, respectively.

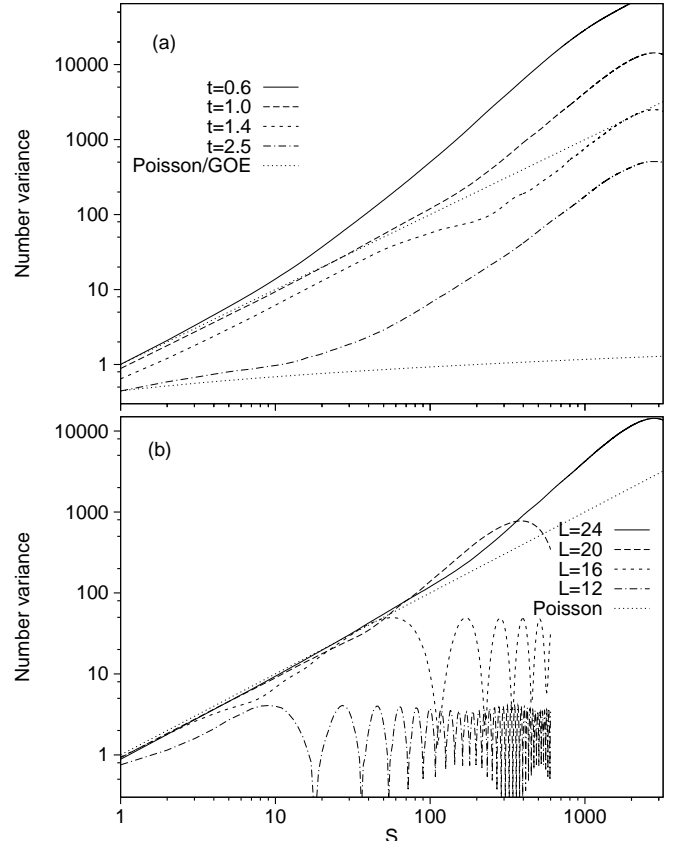


FIG. 7. Number variance $\Sigma^2(S)$ in log-log scale for exactly the same parameters (with an extra data in (b) for $L = 12$) as in previous Figure 6.

B. Matrix elements and integrated conductance

Knowing a complete set of eigenstates in momentum representation, $\langle \vec{k}|n\rangle$, it is easy to compute the matrix elements of the current observable

$$\langle n|J|m\rangle = \sum_{\vec{k}} J_{\vec{k}} \langle n|\vec{k}\rangle \langle \vec{k}|m\rangle. \quad (46)$$

Again, one should make use of translational symmetry (23), since $[S, J] = 0$, to point out that matrix elements are non-vanishing only within a fixed quasi-momentum block, $K_n \neq K_m \Rightarrow \langle n|J|m\rangle = 0$. In order to obtain the numerical results presented in this subsection we averaged over all Fock space (all K), except again for $L = 24, \rho = 1/4$ where we average only over a block with

quasi-momentum $K = 1$. Real part of high-temperature electric conductivity (6) can be (for fixed size L) rewritten as

$$\sigma'(\omega) = \frac{\pi\beta}{L\mathcal{N}} \sum_{n,m} |\langle n|J|m\rangle|^2 \delta_p(\frac{1}{2\pi}(\omega - \phi_m + \phi_n)) \quad (47)$$

In order to avoid awkward smoothing procedure and to simplify the notation we introduce scaled integrated conductivity $I^L(\omega)$

$$\begin{aligned} I^L(\omega) &= \frac{2}{\beta} \int_0^{\omega+0} \sigma'(\nu) d\nu \\ &= \frac{1}{L\mathcal{N}} \sum_{n,m} |\langle n|J|m\rangle|^2 \theta(\omega + 0 - |\phi_m - \phi_n|'), \end{aligned} \quad (48)$$

where $|\eta|' := \min\{|\eta|, 2\pi - |\eta|\}$ and $\theta(x)$ is a Heaviside step function. Integrated conductivity $I(\omega)$ is a monotonically increasing function on the frequency interval $\omega \in [0, \pi]$, starting from the charge stiffness

$$I^L(0) = D_J^L \quad (49)$$

and satisfying the sum-rule on the other end

$$I^L(\pi) = \frac{1}{L} \langle J^2 \rangle^L. \quad (50)$$

Note that the current variance can be computed [15]

$$\frac{1}{L} \langle J^2 \rangle^L = \frac{N(L-N)}{2L(L-1)} = \frac{1}{2}\rho(1-\rho) + \mathcal{O}\left(\frac{1}{L}\right). \quad (51)$$

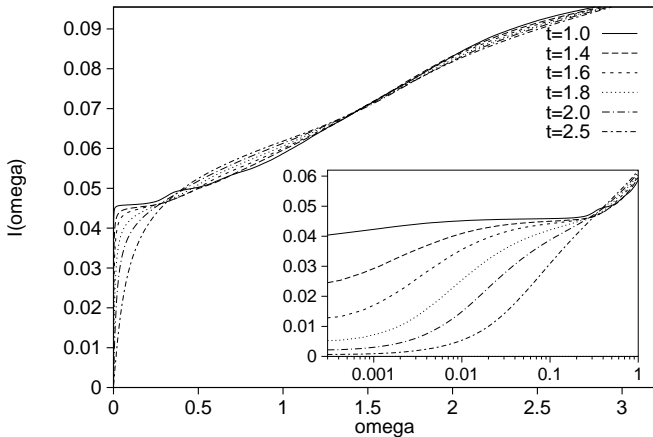


FIG. 8. We show the integrated conductance $I(\omega)$ for a cyclic chain of size $L = 24$ and parameter $V = 2$ and for several different values of parameter t (see legend). In the inset we show the same plot in semi-log scale in order to illustrate the zero frequency jump — the charge stiffness D_J^L .

In Fig.8 we plot the integrated conductivity $I^L(\omega)$ for different values of the kick parameter t (fixed $V = 2$) for constant size $L = 24$ and density $\rho = 1/4$, showing the transition from ergodic $D_J^L \approx 0$ to non-ergodic

$D_J^L > 0$ dynamics, consistent with results of direct time evolution of Sec.III. In Fig.9 we analyze the dependence of $I^L(\omega)$ on size L for fixed values of parameters in non-ergodic regime $t = 1, V = 2, \rho = 1/4$. Note that for small frequencies ω , $I^L(\omega)$ is roughly constant over the frequency interval $0 \leq \omega \leq \omega_*^L$, whose width is determined by the Thouless time of a finite system $\mu(L) \sim L$, namely $\omega_*^L = 2\pi/L$. Note that the expression for stiffness (49) is not completely consistent with the correct definition (8), since the time-limit $\tau \rightarrow \infty$ is implicit in (49) before TL of increasing L can be considered, whereas the correct order of limits is just the opposite. (This proves another advantage of the study of direct time-evolution of Sec.III over the more common frequency-domain approach presented here.)

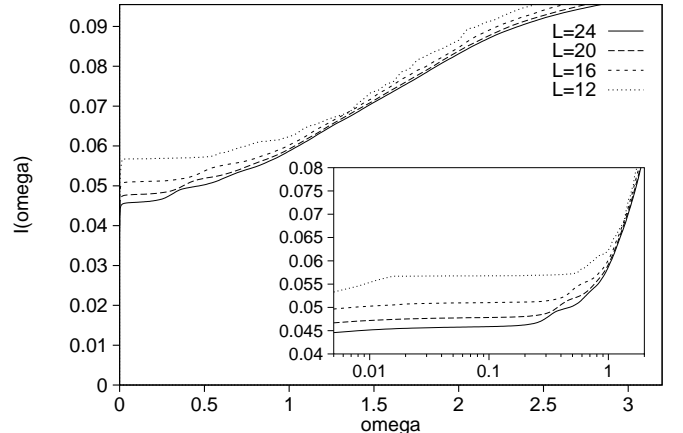


FIG. 9. We show the integrated conductance $I(\omega)$ for a quarter filled $\rho = 1/4$ cyclic chain at $t = 1, V = 2$ (in non-ergodic regime) and for different sizes $L = 24, 20, 16, 12$. In the inset we show the same plot in semi-log scale in order to illustrate the convergence of the charge stiffness. Observe that the size of the horizontal plateau at small frequencies shrinks as $\sim 2\pi/L$.

An interesting conjecture has been put forward in Refs. [9] (and critically debated in [33,34]), namely that half-filled $\rho = 1/2$ integrable t-V model should exhibit properties of an ideal insulator at all temperatures when $V > t$ (in our notation). Insulating behavior is characterized by $D_J^\infty = I^\infty(0) = 0$ and $(2/\beta)\sigma'(0) = (d/d\omega)I^\infty(0) = 0$, so the time correlation function $C_J(\tau)$ should be an oscillatory function in order to integrate to zero.

We have found numerical evidence of (at least approximately) insulating behavior even in the non-integrable half-filled KtV model, when $V > t$. In Fig.10 we demonstrate a double transition from (approximately) insulating regime (example for $t = 0.4, V = 1$) to ideally conducting regime (example for $t = V = 1$) to normally conducting regime (example for $t = 4.5, V = 1$) for a half-filled KtV model on $L = 16$ sites.

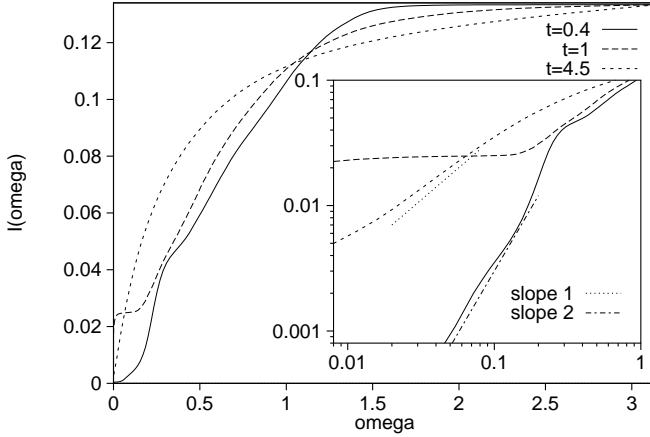


FIG. 10. Integrated conductance $I(\omega)$ for a half-filled ($\rho = 1/2$) cyclic chain of size $L = 16$ is shown for three different values of parameter t (and fixed parameter $V = 1$) demonstrating a double transition from insulator (here for $t = 0.4$) to ideal conductor (here for $t = 1$) to a normal conductor (here for $t = 4.5$) as the kick parameter t is increased. In the inset we show the same three curves in log-log scale.

V. THIRD METHOD: ALGEBRAIC CONSTRUCTION OF TIME-AVERAGED OBSERVABLES FOR INFINITE SYSTEM

A large amount of numerical evidence has been presented in previous two sections in support of the Conjecture put forward in Sec.I. However, all this evidence is based on computations on many-body systems of finite size L , and TL has been speculated by extrapolation to $1/L = 0$. One may still have doubts, that in a non-integrable system that is close to an integrable one quantum ergodicity may squeeze in for large sizes L , beyond the scope of numerical observation. Therefore, as a complementary alternative, one would like to have a method of computation of time-correlators, like D_A (40), which would directly operate with infinite systems on infinite lattices $L = \infty$. In this section we elaborate such a method of computation of operator valued time-average of an observable A in Heisenberg representation

$$\bar{A} = \lim_{M \rightarrow \infty} \frac{1}{2M+1} \sum_{m=-M}^M A(m). \quad (52)$$

The method is specially designed for kicked systems whose propagators can be decomposed in several non-commuting parts [35], and will be implemented to compute time-averaged observables in infinite KtV model, in particular \bar{J} and \bar{T}' , and the corresponding correlators, such as the charge stiffness D_J .

A. Mathematical structures

The first essential mathematical structure used in this section is the Hilbert space of *pseudo-local* quantum observables. Even in the general setting we assume that the evolution propagator preserves the number of particles, $[U, \rho] = 0$. So we again fix the density of particles ρ and consider observables A over a Fock (sub)space of quantum states with a given density parameter ρ . Such observables should also preserve the number of particles, $[A, \rho] = 0$.

Let us define the *scalar product* of two *extensive* observables A and B as

$$(A|B) = \lim_{L \rightarrow \infty} \frac{1}{L} \langle A^\dagger B \rangle_\rho^L = \langle \frac{1}{L} A^\dagger B \rangle_\rho \quad (53)$$

We note that (53) has all the necessary properties of a scalar (inner) product: it is linear in the right factor, positive, and $(A|B) = (B|A)^*$. Note also that averaging over half-filled states is in TL equivalent to the ‘grand-canonical’ average, $\langle \cdot \rangle_{\rho=\frac{1}{2}} \equiv \langle \cdot \rangle$.

The observable A is called weakly local or pseudo-local, if $\|A\|^2 := (A|A) < \infty$. Pseudo-local observables A constitute a Hilbert space denoted by \mathfrak{U} . There is a *linear subspace* $\mathfrak{U}' \subseteq \mathfrak{U}$ of pseudo-local observables A , such that $[A, B] = AB - BA$ is pseudo-local for any pseudo-local $B \in \mathfrak{U}$. For any such $A \in \mathfrak{U}'$, the scalar product (53) is an invariant bilinear form with respect to the *adjoint map* $(\text{ad } A)B = [A, B]$, namely

$$((\text{ad } A^\dagger)B|C) = (B|(\text{ad } A)C). \quad (54)$$

The second essential mathematical structure is the *unitary* Heisenberg-Floquet map $\hat{U}_{\text{ad}} : \mathfrak{U} \rightarrow \mathfrak{U}$, which propagates quantum observables in Heisenberg representation for one period of time, starting at some time $\eta \in [0, 1]$,

$$\hat{U}_{\text{ad}} A(\eta + m) = A(\eta + m + 1) = U^\dagger A(\eta + m)U, \quad (55)$$

$$(\hat{U}_{\text{ad}} A|\hat{U}_{\text{ad}} B) = (A|B). \quad (56)$$

For example, for the KtV model (in spin representation which is, for algebraic convenience, used in this section) we have (19)

$$U|_{\eta=\frac{1}{2}} = \exp(-i\frac{1}{2}tH_1) \exp(-iV(H_0 + \frac{1}{2}S_z)) \exp(-i\frac{1}{2}tH_1) \quad (57)$$

with the potential and kinetic generator

$$H_0 = \frac{1}{4} \sum_{j=-\infty}^{\infty} \sigma_j^z \sigma_{j+1}^z, \quad (58)$$

$$H_1 = \frac{1}{4} \sum_{j=-\infty}^{\infty} (\sigma_j^+ \sigma_{j+1}^- + \sigma_j^- \sigma_{j+1}^+).$$

Unlike in Sec.III, we have here taken the time steps in the middle between the kicks, $\eta = \frac{1}{2}$, in order to fully exploit

the time-reversal symmetry of the problem. Note that the time evolution of observables which are diagonal in momentum representation, like J and T' , is not affected by the shift η of the origin of the stroboscopic map. The Floquet-Heisenberg map can be written explicitly using an exponential of the adjoint map

$$\hat{U}_{\text{ad}} = \exp(i\frac{1}{2}t_{\text{ad}} H_0) \exp(iV_{\text{ad}} H_1) \exp(i\frac{1}{2}t_{\text{ad}} H_0). \quad (59)$$

Since the density ρ (or magnetization $\mathcal{M} = \rho - \frac{1}{2}$ in spin- $\frac{1}{2}$ formulation) is fixed, the total spin S_z generates an irrelevant phase which does not influence the evolution of observables.

Time-average of observable (self-adjoint operator) A (52) is a solution of the fixed-point equation for the Floquet-Heisenberg map

$$\hat{U}_{\text{ad}} \bar{A} = \bar{A}. \quad (60)$$

Time-averaging in operator space can also be written in terms of an orthogonal projector \hat{P}_U onto the null space of $1 - \hat{U}_{\text{ad}}$, namely

$$\bar{A} = \hat{P}_U A, \quad \hat{P}_U = \lim_{M \rightarrow \infty} \frac{1}{2M+1} \sum_{m=-M}^M \hat{U}_{\text{ad}}^m. \quad (61)$$

The property

$$\hat{P}_U = \hat{P}_U^2 \quad (62)$$

is easily proved by writing a time-average limit (61) in an equivalent, Gaussian way

$$\hat{P}_U = \lim_{M \rightarrow \infty} \frac{1}{\sqrt{2\pi}M} \sum_{m=-\infty}^{\infty} \exp(-\frac{1}{2}(m/M)^2) \hat{U}_{\text{ad}}^m.$$

Without loss of generality we will in the following assume that observable A is traceless $\langle A \rangle = 0$, such as J and T' . Note that the generalized stiffness (40) can be written simply as

$$D_A = (A|\bar{A}). \quad (63)$$

B. Time-average from Variational Principle in operator space

Scaled (or normalized) time-average of a self-adjoint operator $A = A^\dagger$, $X = \bar{A}/\|\bar{A}\|$, can be obtained from a *variational principle in operator space*, namely as an extremum (*maximum*) of an action $s(X)$

$$\frac{\delta}{\delta X} s(X) = 0, \\ s(X) = \frac{1}{2}(X|A)(A|X) = \frac{1}{2}|(X|A)|^2 \quad (64)$$

with constraints

$$\|(1 - \hat{U}_{\text{ad}})X\|^2 = (X|(1 - \hat{U}_{\text{ad}}^{-1})(1 - \hat{U}_{\text{ad}})|X) = 0, \quad (65)$$

$$(X|X) = \text{const} < \infty, \quad (66)$$

Namely, eqs. (64-66) imply $X = \alpha \bar{A}$, where $\alpha = \|\bar{A}\|^{-1}$ if X is normalized $(X|X) = 1$. Since constraint (65) is homogeneous the corresponding Lagrange multiplier is diverging. Hence, we suggest to write the constrained variational problem (64,65, 66) in the compact form

$$\lim_{\epsilon \rightarrow \infty} \frac{\delta}{\delta X} s_\epsilon(X) = 0 \Rightarrow X = \alpha \bar{A}, \quad \alpha \in \mathbb{C} \\ s_\epsilon(X) = \frac{1}{2}|(X|A)|^2 - \frac{1}{2}\lambda|\epsilon^{-1}(1 - e^{-\epsilon}\hat{U}_{\text{ad}})X|^2 \quad (67)$$

where λ is another Lagrange multiplier associated with the second constraint (66). Indeed, for small ϵ one may write $s_\epsilon(X) = \frac{1}{2}|(X|A)|^2 - \frac{1}{2}\lambda(A|A) - \frac{1}{2}\lambda(\epsilon^{-1} - \epsilon^{-2})(A|(\hat{U}_{\text{ad}} + \hat{U}_{\text{ad}}^{-1} - 2)|A) + \mathcal{O}(\epsilon)$, so homogeneous constraint (65) is satisfied automatically as $\epsilon \rightarrow 0$. Let us now show that the above variational problem has the correct solution (52). We differentiate the action (67)

$$\frac{\delta}{\delta X} s_\epsilon(X_\epsilon) = (A|X_\epsilon)A - \frac{\lambda}{\epsilon^2}(1 - e^{-\epsilon}\hat{U}_{\text{ad}}^{-1})(1 - e^{-\epsilon}\hat{U}_{\text{ad}})X_\epsilon = 0$$

and write $a = (A|X)$. This equation can be solved explicitly for X_ϵ

$$X_\epsilon = \frac{a\epsilon^2}{\lambda}(1 - e^{-\epsilon}\hat{U}_{\text{ad}})^{-1}(1 - e^{-\epsilon}\hat{U}_{\text{ad}}^{-1})^{-1}A \\ = \frac{a\epsilon^2}{\lambda} \sum_{n=0}^{\infty} \sum_{m=0}^{\infty} e^{-(n+m)\epsilon} \hat{U}_{\text{ad}}^{n-m} A \\ = \frac{a\epsilon^2}{\lambda} \sum_{p=-\infty}^{\infty} A(p) \sum_{q=|p/2|}^{\infty} e^{-q\epsilon} \\ = \frac{a\epsilon^2}{\lambda(1 - e^{-\epsilon})} \sum_{p=-\infty}^{\infty} A(p) e^{-(\epsilon/2)|p|}. \quad (68)$$

In the limit $\epsilon \rightarrow 0$, the last expression (68) is proportional to the time-average

$$X = \lim_{\epsilon \rightarrow 0} X_\epsilon = \frac{4a}{\lambda} \bar{A} \quad (69)$$

Evaluation

$$a = (A|X) = a \frac{4D_A}{\lambda}$$

fixes the value of the Lagrange multiplier

$$\lambda = 4D_A. \quad (70)$$

Unitarity (56) and invariance (60) have the following very important consequence

$$(\bar{A}|\bar{A}) = (A|\bar{A}) = (\bar{A}|A) \quad (71)$$

Assuming that X is non-vanishing so that $(X|X) > 0$, and that X and \bar{A} are *proportional*, one can write

$$\bar{A} = \frac{(X|\bar{A})}{(X|X)}X = \frac{(X|A)}{(X|X)}X. \quad (72)$$

Taking the scalar product of the last equation with A , one obtains a very useful expression for the stiffness

$$D_A = \frac{|(A|X)|^2}{(X|X)}. \quad (73)$$

C. Numerical application

However, the minimization of the functionals (64, 67) in the huge infinitely dimensional operator space \mathfrak{U} is not convenient for practical calculation. Instead, we suggest to estimate the time-averaged observable \bar{A} by solving the variational problem (67) in a finite-dimensional subspace $\mathfrak{M}(A) \subset \mathfrak{U}$. (Galerkin-like approach in operator space). In fact, we devise a special sequence of truncated ‘minimal invariant’ operator spaces $\dots \mathfrak{M}_p(A) \subset \mathfrak{M}_{p+1}(A) \dots \subset \mathfrak{U}$, which in the limit $p \rightarrow \infty$ (after closure) contain the time average \bar{A} . Thus, the solutions X_p of the variational problems (67) on spaces \mathfrak{M}_p should converge to the proper scaled time-average X of observable A .

Let $\mathfrak{s} = \{\alpha H_0 + \beta H_1; \alpha, \beta \in \mathbb{C}\}$ be 2-dim linear vector space spanned by the two generators of motion, H_α , $\alpha = 0, 1$ (58). Let us define the *minimal invariant operator space containing A* , as the closure of products of powers of adjoint generators $\text{ad } H_\alpha$, $\alpha = 0, 1$ on A

$$\mathfrak{M}(A) = \overline{\bigcup_{n=0}^{\infty} (\text{ad } \mathfrak{s})^n A} \quad (74)$$

$\mathfrak{M}(A)$ is indeed the minimal (though infinitely-dimensional in general) operator space containing A with the invariance property

$$\begin{aligned} (\text{ad } H_\alpha) \mathfrak{M}(A) &= \mathfrak{M}(A), \quad \alpha = 0, 1, \\ \hat{U}_{\text{ad}} \mathfrak{M}(A) &= \mathfrak{M}(A), \quad \forall t, V. \end{aligned} \quad (75)$$

It is obvious that $\bar{A} \in \mathfrak{M}(A)$. We now construct the countable basis of the space $\mathfrak{M}(A)$ ordered by the order of locality as follows: We assign an observable $\tilde{H}_{q,c}$ to an *ordered pair* of integers (q, c) , *order* q , and *code* c , $0 \leq c < 2^{q-1}$ with $q - 1$ binary digits c_n , $c = \sum_{n=1}^{q-1} c_n 2^{n-1}$, namely

$$\tilde{H}_{q,c} = (\text{ad } H_{c_{q-1}})(\text{ad } H_{c_{q-2}}) \cdots (\text{ad } H_{c_1})A. \quad (76)$$

Since not all observables $\tilde{H}_{q,c}$ upto a given maximal order $p, q \leq p$, are linearly independent we perform Gram-Schmit orthogonalization w.r.t. the scalar product (53)

$$\begin{aligned} G_{q,c} &= \begin{cases} \tilde{G}_{q,c} / \sqrt{(\tilde{G}_{q,c}|\tilde{G}_{q,c})} & \tilde{G}_{q,c} \neq 0, \\ 0; & \tilde{G}_{q,c} = 0, \end{cases} \\ \tilde{G}_{q,c} &= \tilde{H}_{q,c} - \sum_{(r,b) < (q,c)} G_{r,b} (G_{r,b}|\tilde{H}_{q,c}). \end{aligned} \quad (77)$$

The nonzero observables $G_{q,c}$ form the orthonormal basis of $\mathfrak{M}(A)$. Note that observables $G_{q,c}$ are strictly local operators of order q : in case of spin representation of KtV model they are represented as expansions

$$G_{q,c} = \sum_{s_0, s_1, \dots, s_q} g_{q,c}^{s_0 s_1 \dots s_q} Z_{s_0 s_1 \dots s_q} \quad (78)$$

in terms of spatially homogeneous finite products of field operators

$$Z_{s_0 s_1 \dots s_q} = \sum_{j=-\infty}^{\infty} \sigma_j^{s_0} \sigma_{j+1}^{s_1} \cdots \sigma_{j+q}^{s_q},$$

where $s_k \in \{0, +, -, z\}$ and $\sigma_j^0 = 1$. The (average) number of nonzero terms in expansions (78) was found to grow exponentially at approximately the same rate for both observables under study, J and T' , namely as

$$\#\{g_{q,c}^{s_0 s_1 \dots s_q} \neq 0\} \approx 0.5 \times 2.55^q,$$

which may be further reduced by a factor 2, or even by a factor 4 if $\rho = \frac{1}{2}$, using the symmetries $\hat{\mathcal{P}}$ (24), and $\hat{\mathcal{R}}$ (25) (the latter may be used if $\rho = \frac{1}{2}$). Note that the entire linear space $\mathfrak{M}(A)$ has the same symmetry properties as observable A , for example the space $\mathfrak{M}(J)$ and $\mathfrak{M}(T')$ belong to a negative and positive parity symmetry class, respectively, w.r.t. parity operation (24),

Let us now define a sequence of *truncated minimal invariant operator spaces* containing A ,

$$\mathfrak{M}_p(A) = \overline{\bigcup_{n=0}^{p-1} (\text{ad } \mathfrak{s})^n A}, \quad p = 1, 2 \dots \quad (79)$$

with dimensions $d_p(A) := \dim \mathfrak{M}_p(A)$. Linear space $\mathfrak{M}_p(A)$ contains operators derived from A by composition of generators $\text{ad } H_\alpha$ up to *order* p . Due to binary code construction (76) we have a strict upper bound on the growth of dimensions of the truncated spaces $\mathfrak{M}_p(A)$,

$$d_p(A) \leq 2^{p-1}, \quad (80)$$

however actual dimensions may grow considerably slower (due to systematic linear dependences among $\tilde{H}_{p,b}$), namely for $A = J$ and $A = T'$ we find by computer algebra up to $p = 14$ th order (see Tab.1)

$$d_p(J) \approx 1.825^{p-1}, \quad d_p(T') \approx 1.68^{p-1} \quad (81)$$

Let $\mathbf{H}_{p,\alpha}$, $\alpha = 0, 1$, denote real and symmetric (Hermitian in general) matrices of linear maps $\text{ad } H_\alpha$ on $\mathfrak{M}_p(A)$ with images orthogonally projected back to $\mathfrak{M}_p(A)$. It follows from the construction that they have (generally) a block-banded structure where the blocks correspond to observables with a fixed order q : namely

$$(G_{q,c}|\text{ad } H_\alpha|G_{q',c'}) = 0, \quad \text{if } |q - q'| \neq 1. \quad (82)$$

The truncated adjoint maps, $\mathbf{H}_{p,\alpha}$, have nontrivial null spaces

$$\mathfrak{N}_{p,\alpha}(A) = \{B \in \mathfrak{M}_p(A); [H_\alpha, B] \in \mathfrak{M}_{p+1}(A) - \mathfrak{M}_p(A)\}, \quad (83)$$

with dimensions $d_{p,\alpha}(A) := \dim \mathfrak{N}_{p,\alpha}(A)$ which increase approximately with the same exponent as $d_p(A)$ (81) (see Tab.1).

By means of truncated adjoint maps $\mathbf{H}_{p,\alpha}$ we construct an approximate Floquet-Heisenberg matrix \mathbf{U}_p , which is a $d_p(A)$ -dim *unitary* matrix over the truncated space $\mathfrak{M}_p(A)$

$$\mathbf{U}_p = \exp(i\frac{1}{2}t\mathbf{H}_{p,1}) \exp(iV\mathbf{H}_{p,0}) \exp(i\frac{1}{2}t\mathbf{H}_{p,1}) \quad (84)$$

Now we are ready to solve the variational problem (64-67) in the truncated space $\mathfrak{M}_p(A)$. We note an important ‘experimental’ observation (whose theoretical understanding is still lacking) namely that the matrix $\mathbf{1} - \mathbf{U}_p$ possesses a high-dimensional null-space

$$\mathfrak{N}_p^U(A) = \{B \in \mathfrak{M}_p(A); \mathbf{U}_p B = B\},$$

whose dimension $d_p^U(A) := \dim \mathfrak{N}_p^U(A)$ is, for odd p , independent of parameters t, V and equal to the dimension of the null space of $\mathbf{H}_{p,1}$,

$$d_{2l-1}^U(A) = d_{2l-1,1}(A). \quad (85)$$

Note also that for odd order of truncation $p = 2l - 1$, the elements of null space $B \in \mathfrak{N}_p^U(A)$ are spanned by combinations of *even* powers of generators only, i.e. $(B|G_{2l,c}) \equiv 0$, which is due to time-symmetric construction ($\eta = \frac{1}{2}$) of evolution operator \hat{U}_{ad} (59).

The scalar products (53) for different values of the density ρ are non-degenerate with respect to each other, and therefore the dimensions of various linear (sub)spaces, $d_p(A), d_{p,\alpha}(A), d_p^U(A)$, (see Tab.1) *do not depend* on the density parameter ρ .

| p | $d_p(J)$ | $d_{p,0}(J)$ | $d_{p,1}(J)$ | $d_p(T')$ | $d_{p,0}(T')$ | $d_{p,1}(T')$ |
|-----|----------|--------------|--------------|-----------|---------------|---------------|
| 1 | 1 | 1 | 1 | 1 | 0 | 1 |
| 2 | 2 | 0 | 2 | 2 | 0 | 1 |
| 3 | 4 | 2 | 2 | 4 | 1 | 2 |
| 4 | 7 | 3 | 3 | 6 | 2 | 1 |
| 5 | 12 | 6 | 4 | 10 | 4 | 5 |
| 6 | 21 | 9 | 7 | 15 | 5 | 2 |
| 7 | 38 | 16 | 12 | 25 | 9 | 10 |
| 8 | 69 | 27 | 21 | 40 | 12 | 7 |
| 9 | 126 | 48 | 38 | 66 | 22 | 21 |
| 10 | 230 | 84 | 68 | 107 | 33 | 22 |
| 11 | 419 | 153 | 123 | 178 | 60 | 51 |
| 12 | 763 | 273 | 223 | 293 | 91 | 66 |
| 13 | 1393 | 493 | 409 | 494 | 162 | 137 |
| 14 | - | - | - | 831 | 257 | 202 |

TABLE I. Dimensions of the truncated minimal invariant spaces and of the null-spaces of truncated adjoint maps for different orders of truncation p .

The constraint (65) is now equivalent to restricting the variation (64) to the sub-space $\mathfrak{N}_p^U(A)$. Hence, the ‘truncated’ scaled time-averaged observable X_p is a maximum of the quadratic form $(X_p|A)(A|X_p)$ on $\mathfrak{N}^U(A)$ with a normalization constraint $(X_p|X_p) = 1$. In other words, if $F_n, n = 1, \dots, d := d_p^U(A)$ is an orthonormal basis of the null-space $\mathfrak{N}_p^U(A)$ and if (x_1, \dots, x_d) is a normalized eigenvector of the (positive definite) $d \times d$ matrix eigenvalue problem

$$\sum_n (F_m|A)(A|F_n)x_n = fx_m$$

with the *maximal* eigenvalue f , then

$$X_p = \sum_n F_n x_n. \quad (86)$$

is a solution of the variational problem (64-67) in the truncated space $\mathfrak{M}_p(A)$. In the limit $p \rightarrow \infty$ we expect to recover an exact time-average

$$\lim_{p \rightarrow \infty} X_p = X = \|A\|^{-1} \bar{A}. \quad (87)$$

However, if the system is ergodic, time average should be zero $\bar{A} = 0$ (note that $\langle A \rangle = 0$), so the (normalizable) limit (87) should not exist. In order to inspect the convergence of X in the Hilbert space of observables, we define a *relative norm* $N_q(X)$ w.r.t. order q

$$N_q(X) = \sum_c |(X|G_{q,c})|^2. \quad (88)$$

Since

$$\|X\|^2 = \sum_{q=0}^{\infty} N_q(X), \quad (89)$$

the inspection of the convergence of the sum on RHS of (89) would give us indication of convergence of X (87) and thus non-ergodicity of the problem. As a second criterion of convergence of X we study *stability* of X_p , or of the relative norms $N_q(X_p), q \leq p$, w.r.t. variation of the truncation order p .

In Figs.11,12 we show the relative norms $N_q(X_p)$ of the normalized time-average of the current J (Fig.11) and kinetic energy T' (Fig.12) for several different orders of truncation p (up to $p = 11$ for J and up to $p = 13$ for T'). We note that for both observables, X_p is quite stable against variation of p , for $t \leq 1.4$, and in the same parameter range, the coefficients $N_q(X_p)$ seem to be summable. The stiffness D_A (73) may be re-written in terms of relative norms as

$$D_A = (A|A) \frac{N_1(X)}{\sum_{q=1}^{\infty} N_q(X)}. \quad (90)$$

In this regime where X is convergent in \mathfrak{U} , $N_q(X_p)$ are good approximation of $N_q(X)$ for $q \leq p$ (apart from

a constant renormalization prefactor which cancels out from expressions like (90)), and we may write a good estimate for the upper bound on the stiffness

$$D_A^p = |(A|X_p)|^2 \approx (A|A) \frac{N_1(X)}{\sum_{q=1}^p N_q(X)} \\ > (A|A) \frac{N_1(X)}{\sum_{q=1}^{\infty} N_q(X)} = D_A^{\infty}. \quad (91)$$

However, we would like to have accurate approximations of the stiffness D_A^{∞} itself rather than the accurate upper bounds, so we extrapolate the relative norms $N_q(X) \approx N_q(X_p)$ to orders higher than the order of truncation, $q > p$, in expression for the stiffness (90) by fitting the tail of $N_{q=2l+1}(X_p)$ at three points: $q = p - 4, p - 2, p$ (note that $N_{q=2l}(X_p) = 0$) with exponential ansatz $N_{q=2l+1}(X_p) \propto \exp(-sq)$. Since the actual rate of convergence of $N_q(X) \rightarrow 0$, as $q \rightarrow \infty$ is probably slower than exponential (see Figs.11,12), the stiffness extrapolated in this way (eq. (90)), D_A^e , is probably still slightly overestimated. In Fig.13 we show the dependence of the extrapolated charge stiffness D_J^e on the parameter t (and for fixed $V = 2$) through the critical range $t \sim t_c \approx 1.4$, and compare it with the charge stiffness as computed from direct diagonalization of the finite KtV chains of sizes $L = 24, 20, 16$. When approaching the critical point t_c , the fitted slope s linearly decreases to zero. For larger values of parameters, $t > t_c(V)$, X_p is not stable against variation of p and the partial sums of relative norms $N_q(X)$ are not converging. Therefore, $\bar{A} = 0$ and $D_A^{\infty} = 0$, and the system is quantum ergodic. In Fig.14 we plot a full (t, V) phase diagram of the (extrapolated) charge stiffness D_J^e . It is clear that this last method, since it operates with an infinite system, gives the most reliable results on the critical regions of transition between dynamical phases. However, no other dynamical information on correlation functions is obtained other than their time-averages, so within the present method we cannot make any claims on the stronger ergodic property of quantum mixing.

Although dynamical behavior of observables may depend on the symmetry class of observables w.r.t., say, parity operation (24), we have found very similar ergodic, non-ergodic, and critical regions, for the two examples of opposite parity observables, J and T' , that have been under study. However, we should note that dynamical behavior may also depend on the other (continuous) conserved quantities, such as the density ρ . Our results for other values of density ρ indicate that the transition region between ergodic and non-ergodic dynamics moves to slightly smaller values of parameter t as ρ approaches 1/2. Due to particle-hole transformation (25) the dynamics for $\rho = \rho'$ is equivalent to dynamics for $\rho = 1 - \rho'$.

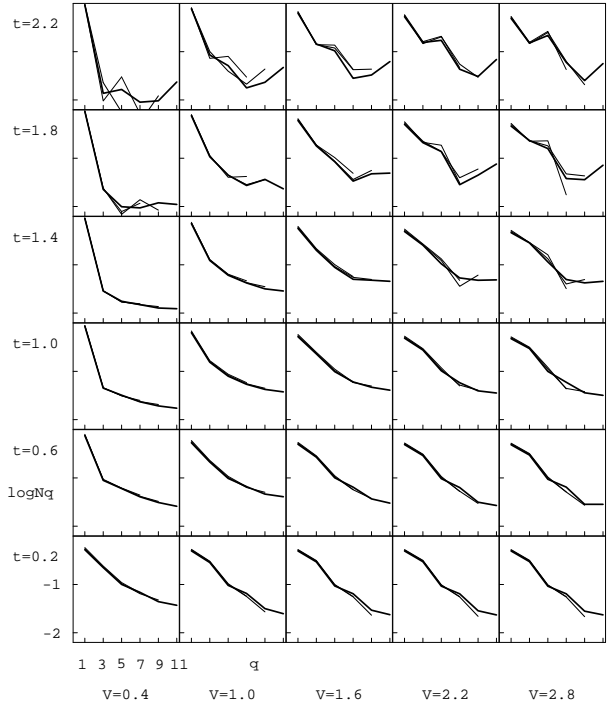


FIG. 11. The logarithm of relative norm $N_q(X)$ of the normalized time-averaged current $X = \bar{J}/\|J\|$ in a quarter-filled ($\rho = 1/4$) infinite KtV model is plotted against (odd) order $q = 2l - 1$, for a square mesh of parameters t and V . The three different curves on each graph, thick, medium, and thin, refer to three different orders of truncation of operator spaces, $p = 11$, $p = 9$, and $p = 7$, respectively.

We should note that in a recent paper [36] a very similar algebraic approach has been used in order to compute the pseudo-local quantum invariants of motion. In the regime of non-ergodic dynamics, one or two, converged pseudo-local invariants of motion were found, whereas in the regime of ergodic dynamics, no non-trivial invariants of motion were found. Then by using a formula (9) of Mazur [11] and Suzuki [12], the time averaged correlation of kinetic energy D_T has been computed by means of an expansion in terms of pseudo-local invariants, giving the results which are in good agreement with the results of direct calculations on finite systems. We believe that our variational approach in the space of observables presented here is (in general, possibly non-integrable case) an improvement of the Mazur-Suzuki approach [11,12] to the calculation of time-averaged correlators. Within Mazur formula (9) one is typically able only to write only inequality (lower bound on stiffness) since the set of *known local* invariants of motion may be *incomplete*.

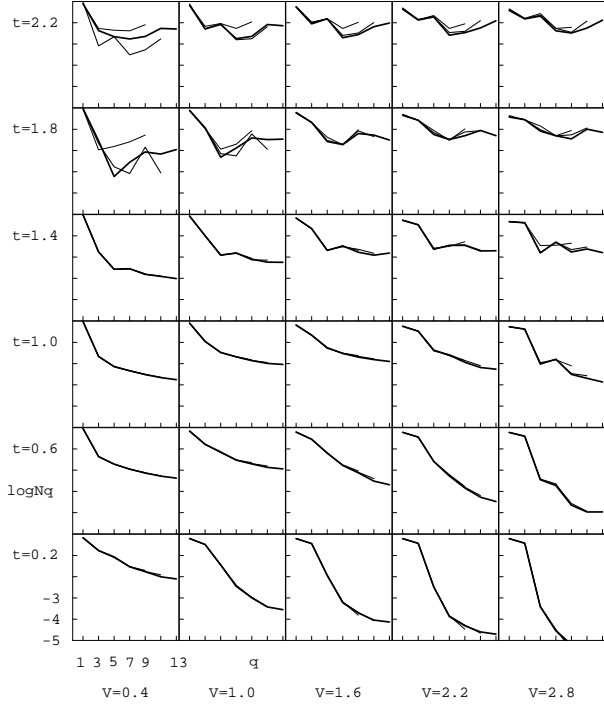


FIG. 12. Same as in previous Fig.11 for the normalized time-averaged kinetic energy $X = \bar{T}'/\|\bar{T}'\|$, except for larger truncation orders, $p = 13$ (thick curves), $p = 11$ (medium curves), $p = 7$ (thin curves).

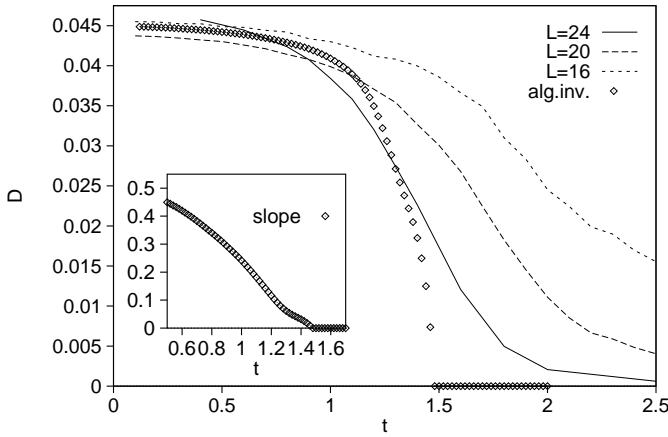


FIG. 13. Charge stiffness D_J vs. kick parameter t and constant parameter $V = 2$ for quarter-filled chain $\rho = 1/4$. Different curves refer to different system sizes $L = 24, 20, 16$, while points represent the infinite-size stiffness (73) based on extrapolated algebraic time-averaged current invariant of motion. The truncation order is $p = 11$. In the inset we show the logarithmic slope s of the falloff of the relative norms $N_q(\bar{J}) \propto \exp(-sq)$ at $q \approx p$.

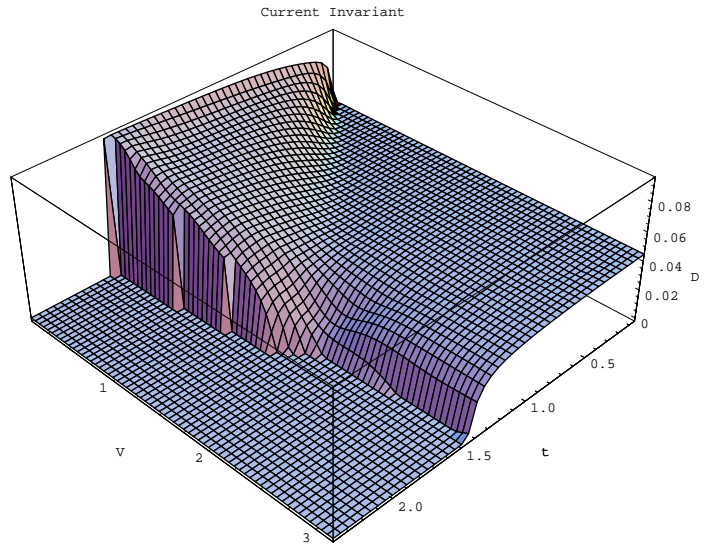


FIG. 14. (t, V) phase diagram of the charge stiffness D_J for quarter-filled ($\rho = 1/4$) infinite KtV model, as deduced from extrapolated time-averaged current \bar{J} .

VI. CONCLUSIONS AND DISCUSSION

In this paper we have presented three complementary (mainly numerical and computer-algebraic) approaches to the dynamics of non-integrable quantum many-body systems in thermodynamic limit (TL), demonstrated and studied in a kicked t-V model of spinless fermions. We have been primarily interested in the structural stability of non-ergodic quantum motion and the transition from non-ergodic/non-mixing to ergodic/mixing dynamics in TL.

The first approach that we have used is a direct time-evolution of a finite quantum system (which may be in the present model performed very efficiently by means of the so-called Fermionic Fast Fourier Transformation) and computation of time-correlation functions of generic quantum observables. The size L of the system is systematically increased and TL is speculated based on extrapolation to $1/L = 0$. For sufficiently large values of kick parameters, we have found quantum mixing and *exponential* decay of time correlation functions, while for smaller, intermediate values (~ 1) of kick parameters, we have found non-mixing quantum motion characterized by saturating, non-vanishing time-correlation functions.

Our second approach is a direct diagonalization of the stationary quantum problem of finite size and calculation of dynamical properties, such as charge stiffness, conductivity, etc., in frequency domain. Also traditional quantum signatures of chaos, such as level statistics, has been inspected and shown to correspond with the dynamical behavior. This approach is less computationally efficient in case of the present model than the first one.

In the third approach, which is fully complementary to the other two, we propose a method for computation of time-averaged observables of an infinite system.

Thus we can make most precise statements on quantum-ergodicity of an infinite system, which are in complete agreement with the extrapolated results of calculations on finite systems.

The above results are claimed to be the evidence for the validity of the Conjecture (Sec.I), namely that the generic quantum-many-body system in TL may not be quantum-ergodic (or mixing) if it is sufficiently close to an integrable system in parameter space. Recent numerical results on transport in extended (non-integrable) Hubbard model [33] are compatible with the above Conjecture. The transition between non-ergodic and ergodic-dynamics when the external parameters are increased has the properties of (dynamical) phase transition and should be further studied theoretically. First such attempt has been undertaken in [37], where a discretized non-integrable quantum field model (in the continuum limit) has been mapped on a quantum chaotic model of a single particle on a 2-dim torus (in the quasi-classical limit), and the transition from non-ergodic/non-mixing dynamics to ergodic/mixing dynamics of the quantum field model has been identified with the stochastic transition from regular to chaotic motion.

We also give a clear evidence on the non-trivial existence of *mixing quantum motion* in KtV model in TL with *exponentially* decreasing time-correlation functions, provided the external (kick) parameters are large enough (above the critical values). Such quantum mixing behavior may be a source of truly *chaotic* and *macroscopically irreversible* quantum motion of many-body systems [38]. Note that macroscopic irreversibility as a consequence of *non-dissipative* but strongly non-integrable quantum many-body dynamics has been recently observed experimentally [39].

One might doubtfully argue that our quite surprising finding on structurally stable non-ergodic quantum motion in TL (formulated as Conjecture in Sec.I) may be just another peculiarity of Physics in One-dimension, and as such should not be expected to hold in interacting quantum systems in more than one spatial dimension. Being aware of this fear we have straightforwardly extended our KtV model (10,11) to a rectangular periodic $L_1 \times L_2$ lattice in two spatial dimensions, with isotropic hopping in two orthogonal directions and δ -kicked isotropic nearest neighbour interaction. An efficient direct time evolution of the 2-dim KtV model has been implemented analogously along the lines described in Sec.III, and its time correlation functions have been computed accordingly, however due to greater computational complexity only for relatively small lattices of sizes up to 6×5 . We should stress that we were again able to identify quite clearly the two regimes of quantum motion which have been roughly stable against the variation of the lattice size, namely: (i) a quantum mixing regime for sufficiently large t and V , and more important, (ii) quantum non-ergodic and non-mixing regime for $|t| \sim |V| \sim \frac{1}{2}$ (or smaller), although the system is not known to be analytically integrable in the limit $t \rightarrow 0, V \rightarrow 0$. Therefore,

this result (whose details will be published elsewhere) is a small piece of evidence for the validity of our Conjecture in a generic example in two dimensions.

Discussions with Prof. P. Prelovšek, and the financial support by the Ministry of Science and Technology of R Slovenia are gratefully acknowledged.

- [1] I. Kornfeld, S. Fomin and Ya. Sinai, ‘Ergodic Theory’, (Springer 1982)
- [2] V.I. Arnold and A. Avez, ‘Ergodic Problems of Classical Mechanics’ (Benjamin, New York 1968).
- [3] M. Hénon, in ‘Chaos and Quantum Physics’, Les Houches 1989 Proceedings, (Elsevier 1991)
- [4] G. Gallavotti and E.G.D. Cohen, Phys.Rev.Lett. **74**, 2694 (1995), and J. Stat. Phys. **80**, 931 (1995); S. Lepri, R. Livi and A. Politi, Phys.Rev.Lett. **78**, 1896 (1997), and Physica D *in press*.
- [5] We would like to demonstrate statistical laws with the minimal external randomness. Hence we think of an isolated system left to evolve with no contact with thermal reservoirs, since we would like to inspect how non-linear interaction alone can control the ergodic properties of dynamics.
- [6] G. Jona-Lasinio, C. Presilla, Phys.Rev.Lett. **77**, 4322 (1996); P. Castiglione, G. Jona-Lasinio and C. Presilla, J. Phys. A: Math. Gen. **29**, 6169 (1996).
- [7] V.V. Flambaum, F. Izrailev and G. Casati, Phys.Rev.E **54**, 2136 (1996); V.V. Flambaum, A.A. Gribakina, G.F. Gribakin, I.V. Ponomarev, ‘Interaction-Driven Equilibrium and Statistical Laws in Small Systems. The Cerium Atom’, preprint cond-mat/9711213.
- [8] G. Montambaux, D. Poilblanc, J. Bellisard, C. Sire, Phys.Rev.Lett. **70**, 497 (1993); D. Poilblanc, T. Ziman, J. Bellisard, F. Mila, and G. Montambaux, Europhys.Lett. **22**, 537 (1993); T.C. Hsu and J.C. Angles d’Auriac, Phys.Rev.B **47**, 14291 (1993).
- [9] X. Zotos and P. Prelovšek, Phys.Rev.B **53**, 983 (1996); H. Castella, X. Zotos, and P. Prelovšek, Phys.Rev.Lett. **74**, 972 (1995).
- [10] R. Kubo, J. Phys. Soc. Japan **12**, 570 (1957).
- [11] P. Mazur, Physica **43**, 533 (1969).
- [12] M. Suzuki, Physica **51**, 277 (1971).
- [13] X. Zotos, F. Naef, and P. Prelovšek, Phys. Rev. B **55**, 11029 (1997).
- [14] Precise conditions on the “generic” class of interactions are yet to be determined, here we show the conjecture for a particular specific example and quote few other results (Sec. VI). However, we should stress that we have in mind only purely *deterministic systems* and nonrandom interactions, so Hamiltonians H_λ of infinite systems are supposed to be prescribed using a *finite* amount of information.
- [15] T. Prosen, Phys.Rev.Lett. **80** (1998) 1808.
- [16] V.E. Korepin, N.M. Bogoliubov and A.G. Izergin, ‘Quantum Inverse Scattering Method and Correlation Func-

tions', (Cambridge University Press 1993).

[17] M. Gutzwiller, 'Chaos in Classical and Quantum mechanics', (Springer-Verlag, New York 1990); F. Haake, 'Quantum Signatures of Chaos' (Springer-Verlag, Berlin-Heidelberg 1991); G. Casati and B. Chirikov, eds., 'Quantum Chaos: Between Order and Disorder', (Cambridge University Press 1994).

[18] P. Jordan and E. Wigner, *Z. Physik* **47** (1928), 631.

[19] G. Casati, B.V. Chirikov, F.M. Izrailev, and J. Ford, in 'Stochastic Behavior in Classical and Quantum Hamiltonian Systems', Vol.93 of Lecture Notes in Physics, G. Casati and J. Ford, eds. (Springer, New York 1979).

[20] R. Artuso, G. Casati, F. Borgonovi, L. Rebuzzini, and I. Guarneri, *Int.J.Mod.Phys. B* **8**, 207 (1994).

[21] W.H. Press, S.A. Teukolsky, W.T. Vetterling, and B.P. Flannery, *Numerical Recipes*, 2nd ed. (Cambridge University Press, 1992).

[22] S. Winograd, 'Arithmetic Complexity of Computations', (SIAM, Philadelphia 1980).

[23] O. Bohigas, M.-J. Giannoni, and C. Schmit, *Phys.Rev.Lett.* **52**, 1 (1984).

[24] O. Bohigas, in Ref. [3].

[25] A.V. Andreev, O. Agam, B.D. Simons, and B.L. Altshuler, *Phys.Rev.Lett.* **76**, 3947 (1996).

[26] M.L. Mehta, 'Random Matrices' (Academic Press, London 1991).

[27] M.V. Berry and M. Tabor, *Proc. Roy. Soc. London A* **156**, 375 (1977).

[28] M.V. Berry and M. Robnik, *J. Phys. A: Math. Gen.* **17**, 2413 (1984).

[29] T. Prosen and M. Robnik, *J. Phys. A: Math. Gen.* **27**, 8059 (1994).

[30] E.B. Bogomolny *et al*, preprint.

[31] D. Braun, G. Montambaux and M. Pascaud, 'Boundary conditions at the mobility edge', preprint, cond-mat/9712256.

[32] M.V. Berry, *Proc.R.Soc.London A* **400**, 229 (1985).

[33] Kirchner S, Evertz H G and Hanke W 1998 'Transport Properties of One-Dimensional Hubbard Models', preprint, cond-mat/9804148.

[34] S. Fujimoto and N. Kawakami, *J. Phys. A: Math. Gen.* **31**, 465 (1998); N.M.R. Peres, P.D. Sacramento, D.K. Campbell, and J.M.P. Carmelo, 'Curvature of Levels and Charge Stiffness of One-Dimensional Spinless Fermions', preprint, cond-mat/9804169.

[35] The simpler and perhaps more powerful version of the method for the autonomous Hamiltonian systems, which may be used also to give rigorous upper bounds on charge or spin stiffness etc., will be presented elsewhere.

[36] T. Prosen, *J. Phys. A: Math. Gen.* **31** (1998) in press.

[37] T. Prosen, 'A Map from Quantum Field Theory to Quantum Chaos on a 2-dim Torus', preprint 1998.

[38] T. Prosen, G. Usaj and H.M. Pastawski, in preparation.

[39] G. Usaj, H.M. Pastawski and P.R. Levstein, 'Dynamically Driven Irreversibility in Many Body Quantum Systems: An experimental approach', preprint cond-mat/9803047.